

AN AUTOMATIC CROWD-HOIST REGULATOR

FOR THE STRIP MINING INDUSTRY

by

William Albert DeLorme

Thesis submitted to the Graduate Faculty of the

Virginia Polytechnic Institute

in candidacy for the degree of

MASTER OF SCIENCE

in

Electrical Engineering

APPROVED:

Chairman, Dr. M. H. Hopkins

Professor E. A. Manus

Professor R. R. Wright

Dr. R. H. Miller

May, 1966
Blacksburg, Virginia

II. TABLE OF CONTENTS

	Page
I. TITLE PAGE	1
II. TABLE OF CONTENTS	2
A. <u>List of Figures</u>	4
III. INTRODUCTION	6
IV. REVIEW OF LITERATURE	14
V. INVESTIGATIONS	27
A. <u>Development of Motion Transfer Functions</u>	27
1. Hoist Transfer Function G_f	33
2. Hoist Transfer Function $\frac{I_h}{T_h}$	36
3. Crowd Transfer Function $\frac{\omega c}{E_c}$	38
B. <u>Development of Crowd-Hoist Circuits</u>	40
1. The H_t Feedback Network	41
2. The H_{ch} Feedback Network	51
a. Defining the H_{ch} Network	51
b. Development of H_{ch1} and H_{ch2}	60
VI. DISCUSSION OF RESULTS	70
A. <u>Summary of Procedures</u>	70
B. <u>Bode Analysis of System GH</u>	75
VII. ACKNOWLEDGEMENTS	88
VIII. BIBLIOGRAPHY	89

	Page
IX. VITA	91
X. APPENDICES	92
1. Analysis of Mechanical System	93
2. Analysis of System H_t	98
3. H_t Time Domain Linear Response	102
4. General Form of Motion Transfer Functions	106

List of Figures

Figure	Page
1. The Dynamics of a "Knee Action" Shovel	8
2. Simplified Block Diagram for Hoist or Crowd Motion . . .	10
3. Ward-Leonard Loop Volt-Amp Curve	11
4. Block Diagram of Motor and Mechanical System	16
5. Simplified Model of Figure 4	17
6. Motion Voltage Regulator with H_I and H_t	19
7. Result of Adding Feedbacks from ω_M	20
8. Simplified Model of Crowd-Hoist Regulator	23
9. Further Block Reduction of Figure 7	24
10. Resolution of $\frac{\Delta I_h}{\Delta T_L}$	25
11. Crowd-Hoist Regulator	28
12. Crowd or Hoist General Block Diagram	30
13. H_t Feedback Network $\frac{\Delta H_{to}}{\Delta V_t}$	42
14. H_t Feedback Circuits	43
15. Model of Crowd-Hoist Regulator	52
16. H_{ch} Feedback Network $\frac{\Delta E_c}{\Delta I_h}$	53
17. H_{ch1} Feedback Circuit $\frac{\Delta CH_1}{\Delta I_h}$	61
18. H_{ch2} Feedback Circuits $\frac{\Delta CH_2}{\Delta H_{cho}}$	64

Figure	Page
19. System $ GH(j\omega) $ vs ω	83
20. System $\angle GH(j\omega)$ vs ω	84
21. Mechanical System - Force	94
22. Mechanical System - Torsional	94
23. H_t Feedback Network $\frac{\Delta H_{to}}{\Delta \omega_M}$	99
24. H_t Branch Circuit Model	103

III. INTRODUCTION

The object of the investigations detailed in this thesis is to establish certain design criteria for a number of special components which were necessary to the final development of the Strip Mining Industry's first automatic Crowd-Hoist Regulator.

Since it would be impertinent to assume the reader to have an intimate knowledge of Stripping Shovel Control Systems it is only fitting and proper that at this point a brief period is spent surveying the basic concepts of this rather special field.

The two basic mining techniques presently employed are shaft mining and strip mining. The particular technique used depends on the geological conditions encountered; the main considerations being the depth of "overburden" and the thickness of the mineral seam. The "overburden" is simply all the material (dirt, rock, etc.) which overlays the mineral seam itself.

In shaft mining, shafts are cut through the overburden and into the mineral seam. This means of course that men and equipment must be sent down to excavate the mineral, which must then be sent up to the surface. Now, if the thickness of the mineral seam is less than the underground shaft height requirements for men and equipment, a great deal of the material excavated underground is not the mineral sought. This means that since underground excavation is per se much more expensive than surface excavation, the thickness of the mineral seam is of utmost importance.

Strip mining on the other hand employs surface excavation solely. The function of the Stripping Shovel is to excavate strips of overburden, thereby laying bare the geological mineral seam which may then be excavated by other smaller shovels.

The depth of overburden is the main restriction of strip mining. This is made clear by reference to figure 1. Since the stripping shovel's crawlers lie on the top of the mineral seam, the maximum height excursion of the dipper is restricted by the height of the boom.

Thus the choice of which to use, strip or shaft mining is governed in many cases by the economics of the situation --- as most engineering decisions must be in the final analysis. It is of course, the aim of manufacturers of underground mining excavators to design and build their equipment to economically mine a thin seam, and conversely surface mining excavator manufacturers endeavor to design their stripping shovels to handle a greater depth of overburden. This economic philosophy in the last 20 years has led to the evolution of the massive behemoths of the strip mining industry, which today from the floor of a 200 foot deep chasm can gouge 200 cubic yards of overburden at a single bite and then deposit this dipper load on the lip of its self-made chasm.

The rather simplified drawing of figure 1 will be used to explain the basic dynamics of the "knee action" stripping shovel.

The two main parts of the Stripping Shovel's duty cycle are "loading" the dipper and then "spilling" this dipper load of over-

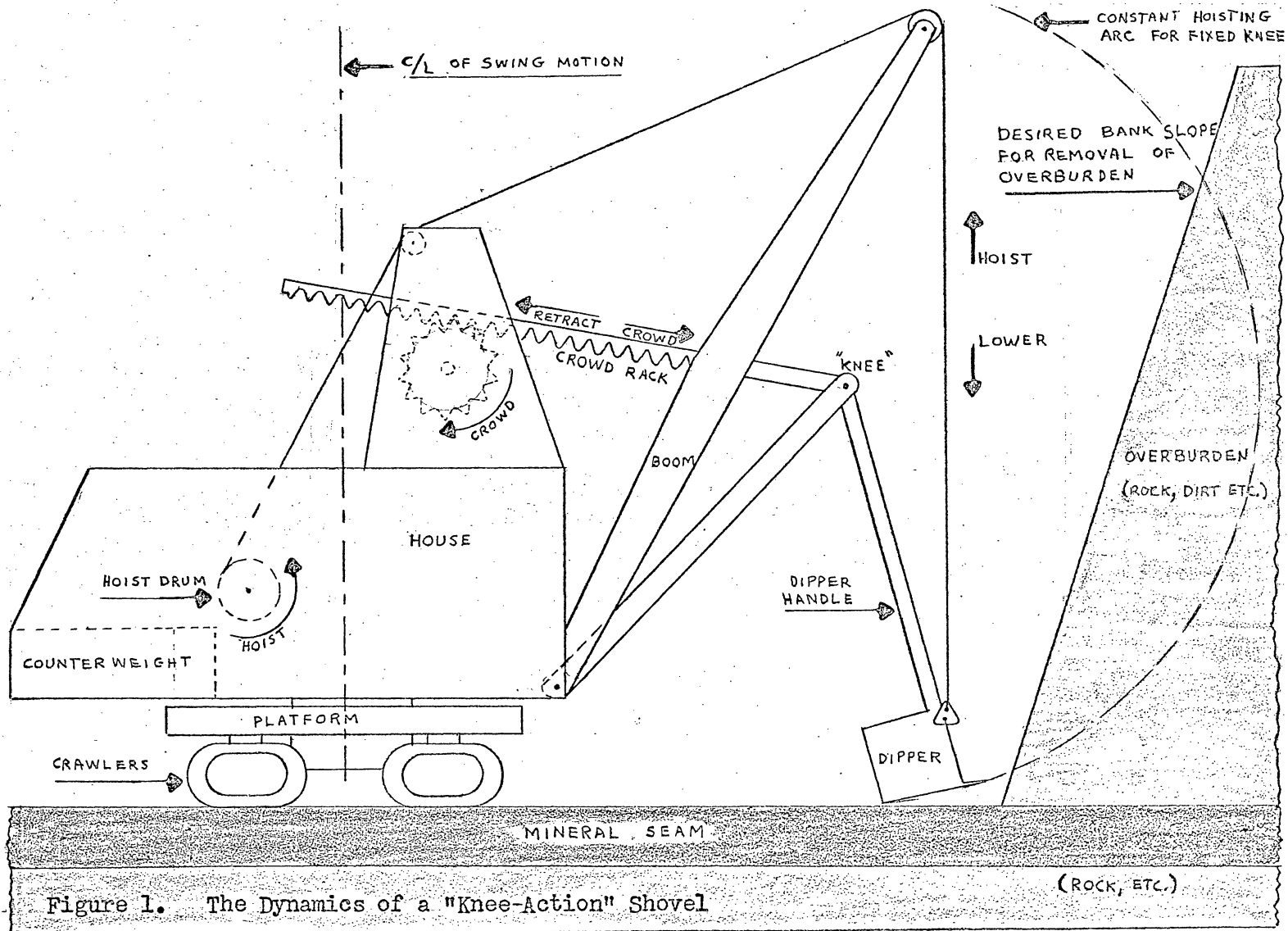


Figure 1. The Dynamics of a "Knee-Action" Shovel

burden on the spoil pile which forms the ridge of its canyon.

It is assumed that the centerline of the "house" remains fixed with respect to the earth, or in other words that the crawlers have propelled the shovel to the face of "overburden" forming the dead-end of the canyon. This position will then allow sequential stripping of the overburden bank.

The "swing" motion allows rotation of the entire shovel (with fixed crawler position), about the centerline running vertically through the "house" as shown in figure 1. Therefore, the swing motion determines the vertical plane in which the dipper will operate. Once the swing position is fixed, the crowd and hoist motions interdependently determine the dynamic dipper location at any instant during a particular dipper loading operation.

Since this thesis is primarily concerned with the shovel dynamics involved in the dipper loading operation, the prime interest is this interdependence of the hoist and crowd motions.

Both the hoist and the crowd motions are closed loop, feedback regulated systems. Figure 2 is a simplified block diagram which applies to either motion, and identifies each motion as a Voltage Regulator with current limit. Each motion derives its respective mechanical power from DC motors and generators arranged in the standard Ward-Leonard configuration. Essentially speed control is obtained by varying the generator voltage as a function of the voltage regulator reference as shown in figure 2.

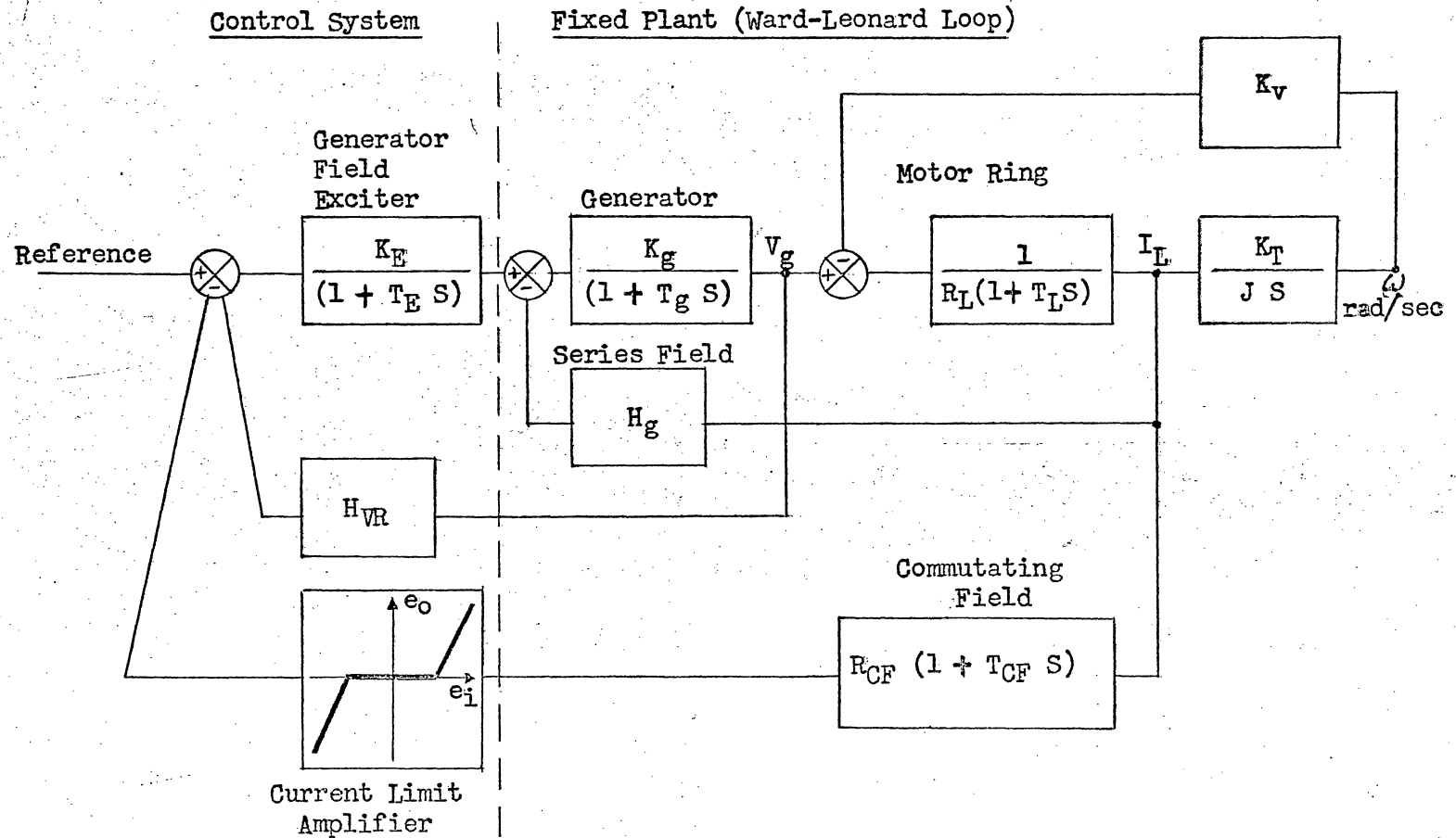


Figure 2. Simplified Block Diagram for Hoist or Crowd Motion

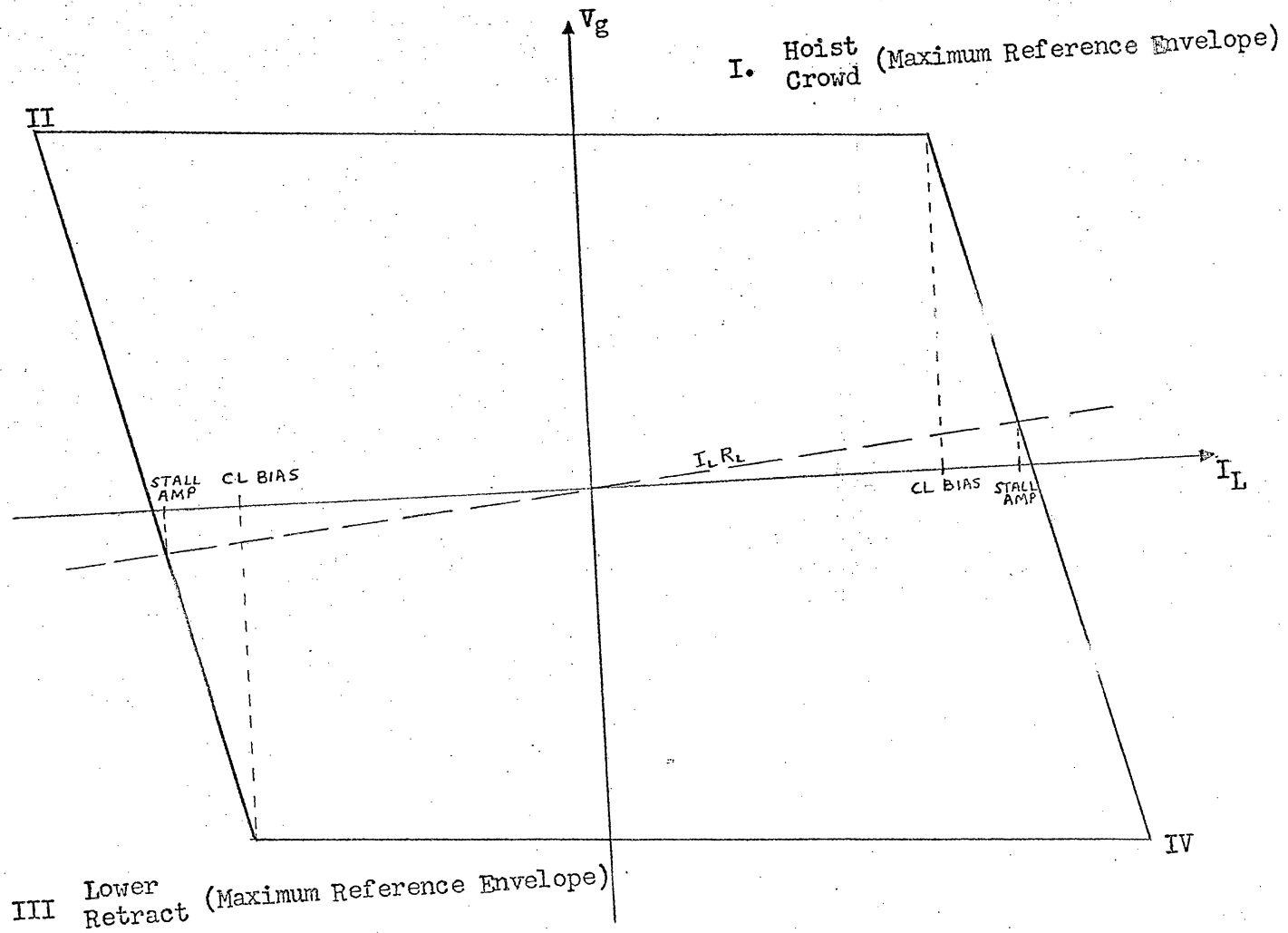


Figure 3. Ward-Leonard Loop Volt-Amp Curve

The voltage regulator with current limit has a static volt-amp curve for the WL loop as shown in figure 3. This type of regulator allows the WL loop current to vary unrestricted within desired machine limits as set by the dead-space in the current limit amplifier as shown in figure 2 and reflected in the volt-amp curve figure 3. Thus, if the loop current should begin to exceed the operating limits of the equipment, the current limit feedback circuit will override the voltage regulator by forcing the reference summing junction towards zero.

The shovel operator seated in the cab has complete and independent control of each motion with a stepless manual controller which provides the voltage regulator reference for that motion.

Now, with the brief descriptions of the hoist and crowd motions just given, consider figure 1 and reflect on the manual dexterity and visual acuity required of the shovel operator during the dipper loading operation.

As shown in figure 1, the dipper will start low to the ground, and teeth into the bank with about equal hoist and crowd reference. Now, as the teeth start into the bank, the operator will tend to "retract" (apply negative crowd reference) while allowing the natural constant hoisting arc to pull the dipper around and set the slope of cut through the bank. As the dipper comes up through the bank as shown on figure 1, the operator will change from a predominately retract to predominately crowd reference, as the dipper handle and crowd rack comes into line at the knee. This sequence of events outlines

one dipper loading operation.

The desired slope of the bank for the removal of overburden, as shown on figure 1 is important for two reasons,

- 1) Any given overburden material has a natural slope which it can hold without sliding.
- 2) If the operator allows a simple constant hoisting arc (i.e. with no crowd motion effort), he would undercut the bank as shown on figure 1 which again encourages sliding.

Now, if the sequence of manual operations required for just one dipper loading is multiplied by the hundreds of dipper loadings performed per work shift, it becomes clear how an automatic dipper loading control can save time and shovel operator fatigue, and both of these factors directly influence the economics of the mining operation.

This concludes a brief outline of the purpose and need for an "automatic crowd-hoist regulator".

IV. REVIEW OF LITERATURE

Because of the uniqueness of the automatic crowd-hoist regulator, to the author's knowledge the only analytical work which has been done in this area is that of Dr. K. G. Black and Mr. M. A. Neslin of the General Electric Schenectady headquarters operation. Mr. M. A. Neslin, who is the Systems Application Engineer for the Strip Mining industry, has influenced greatly the analytical work undertaken in this industry over the last ten years. Dr. K. G. Black is associated with the Systems Analytical section. Together, over the past four years, they have done a great deal of analytical work in the specific area of interest of this thesis, which is incorporated in the GE publication, "Crowd-Hoist Automatic Regulator Interim Report" under #DF-64-AD-36 Technical Information Series.⁽¹⁾

The results of this report outline the analytical requirements of an automatic crowd-hoist regulator which drives the crowd motion as a function of the hoist armature current signal to allow automatic operation of the dipper loading cycle.

The remainder of this section will devote itself to a review of those essential analytical requirements which are necessary to the control system design as the system itself is presently visualized.

Section G of this report presents an analysis of the mechanical oscillations which are present in the Hoist system due to the interactions between the Hoist drive (Hoist motor, gears and drum) and

the driven mass (dipper and dirt). These two masses interact through the hoist rope.

An interesting analog for this mechanical system is derived based on the properties of a torsion pendulum, the analog being two interacting masses connected by a slightly elastic shaft. Appendix 1 derives Dr. Black's analytical expressions from the basic mechanical system. As given by Dr. Black, the spring torsion constant or more accurately the moment of torsion of the shaft (K_r) is given by,

$$K_r = \omega_o^2 \frac{J_M J_L}{J_T} \quad 4.1$$

where, ω_o = angular frequency of oscillation

J_M = motor inertia

J_L = load inertia referred to the motor

$J_T = J_M + J_{L_L}$

therefore,

$$\omega_o^2 = \frac{K_r J_T}{J_M J_L}$$

Based on this analog, the mechanical system including the hoist motor is represented in the more usual system block diagram format in figure 4.

This block diagram is then resolved, figure 5, into a form more easily adapted to the system analysis which will be done. The system oscillatory transfer functions given on figure 5 as G_b and G_g

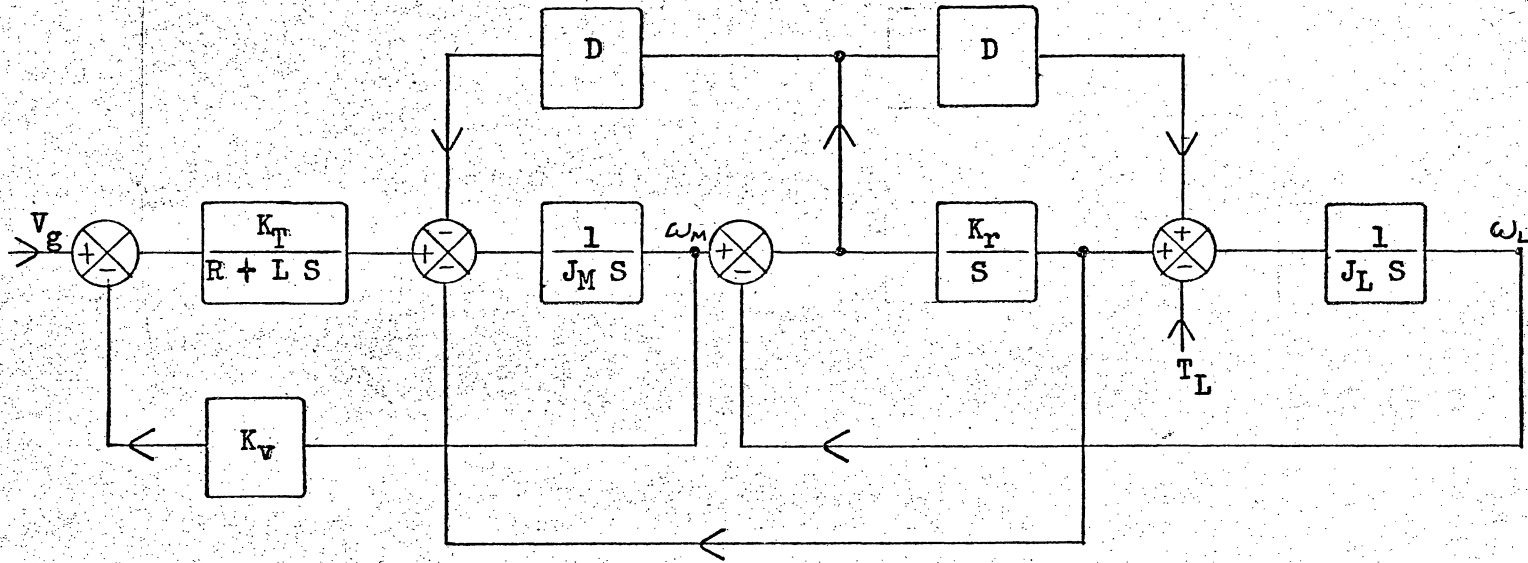


Figure 4. Block Diagram of Motor and Mechanical System

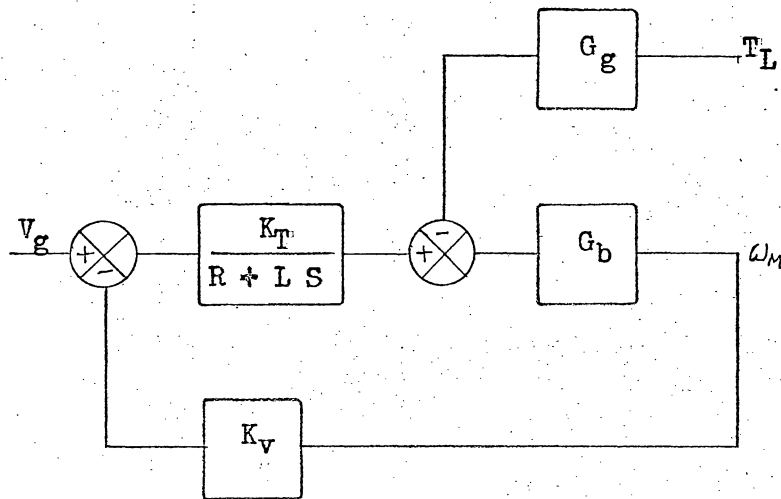


Figure 5. Simplified Model of Figure 4

$$4.3 \quad G_g = \frac{1 + \frac{D}{K_r} s}{1 + \frac{D}{K_r} s + \frac{J_L}{K_r} s^2}$$

$$4.2 \quad G_b = \frac{1}{J_T s} \frac{1 + \frac{D}{K_r} s + \frac{J_L}{K_r} s^2}{1 + \frac{D}{K_r} s + \frac{J_L J_M}{K_r J_T} s^2}$$

should receive particular note.

Sections H and J consider the properties of a tachometer positive feedback network which is shown to be very helpful in stabilizing an oscillatory mechanical system of the type shown in figures 4 and 5.

Figure 6 is a generalized block diagram of the entire Hoist motion utilizing figure 5. In this block diagram, or for that matter throughout the study, the hoist motion is considered to be in current limit, and operating only in the first quadrant of its volt-amp curve (figure 3). Therefore, the current limit amplifier representation shown in figure 2 is not in its dead-space or zero gain region. The negative feedback network H_I includes all resolved elements of armature current feedback to the voltage regulator reference summing junction. The forward gain block G_f is essentially the resolved C/R of the voltage regulator with its output being generator voltage V_g . The positive feedback element H_t is the tachometer feedback referred to above.

The two feedbacks from ω_M are now combined in figure 7 in order to establish the definition of H_t in terms of the other known system parameters.

Now, Dr. Black establishes the following identity which will tend to minimize the effects of the mechanical system oscillations occurring at angular frequency ω_0 ,

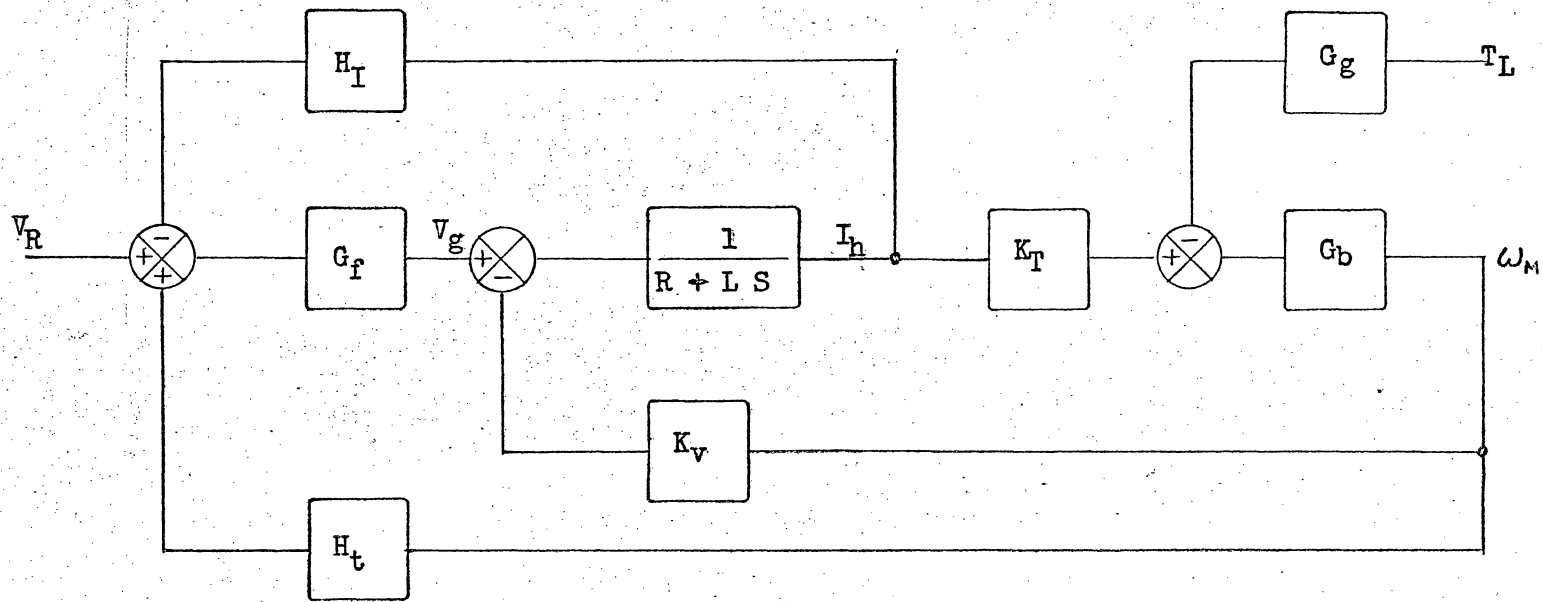


Figure 6. Motion Voltage Regulator with H_I and H_t

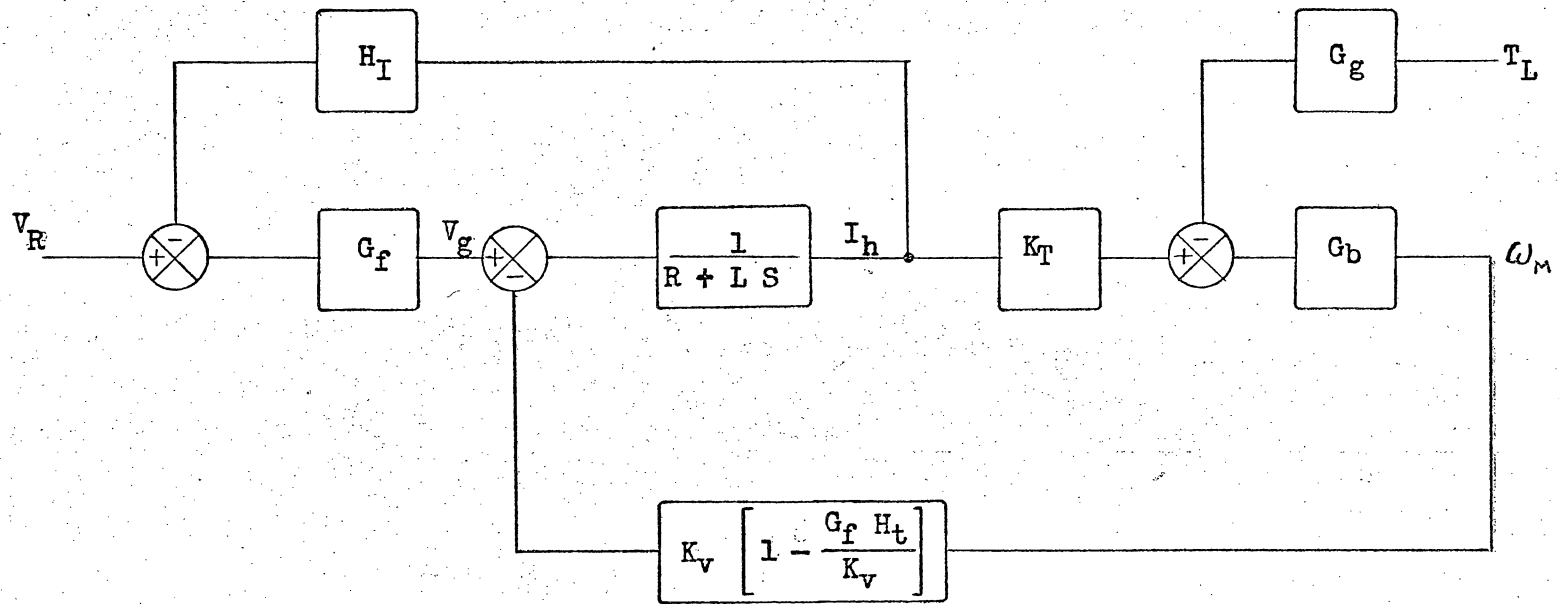


Figure 7. Result of Adding Feedbacks from ω_M

let,

$$K_v \left[1 - \frac{G_f H_t}{K_v} \right] = K_v \left[\frac{1 + \frac{D}{K_r} s + \frac{J_M J_L}{K_r J_T} s^2}{(1 + T_o s)^2} \right]$$

further let,

$$\frac{D}{K_r} = 2\zeta_1 T_o \quad 4.4$$

and let,

$$\frac{J_M J_L}{K_r J_T} = T_o^2 \quad 4.5$$

where,

$$T_o = \frac{1}{\omega_o}$$

therefore,

$$1 - \frac{G_f H_t}{K_v} = \frac{1 + 2\zeta_1 T_o s + T_o^2 s^2}{(1 + T_o s)^2}$$

yielding for H_t ,

$$H_t = \frac{K_v (1 - \zeta_1) 2T_o s}{G_f (1 + T_o s)^2} \quad 4.6$$

This expression will be used extensively in the development of the tachometer feedback network, in particular see section V B 1 and, Appendices 2 and 3.

Sections N and O are the heart of the development of the simplified model of the automatic Crowd-Hoist regulator which applies

to the system as presently visualized. This model is shown in figure 8 and each block will be defined separately.

The block labeled "Hoist" is the resolved transfer function of the Hoist motion from the input T_L to the output I_h . Figures 9 and 10 show by sequential reduction of figure 7 how the transfer function I_h/T_L is obtained.

The Crowd motion is assumed not to be in current limit, and further is allowed to operate in all quadrants of its volt-amp curve as shown in figure 3. Therefore, the "Crowd" block is simply the crowd motion transfer function from its input E_c (crowd error) to its output ω_c . It is evident from figure 2 how the crowd motion transfer function ω_c/E_c is obtained by standard block reduction techniques. If further explanation is desired at this point see section V A 3.

The K_b block represents the effects of the bank as a straight gain term. This assumption was borne out as a good first order approximation by the results obtained from several field tests and is accepted here prima facie.

The block identified as H_{ch} is the Crowd-Hoist feedback network from hoist armature current to crowd error, and as such there are two very important properties to the crowd-hoist regulating scheme which it must contribute in accordance with Dr. Black's analysis. First, it follows from figure 8 that the GH of the automatic crowd-hoist regulator is simply the product of the individual

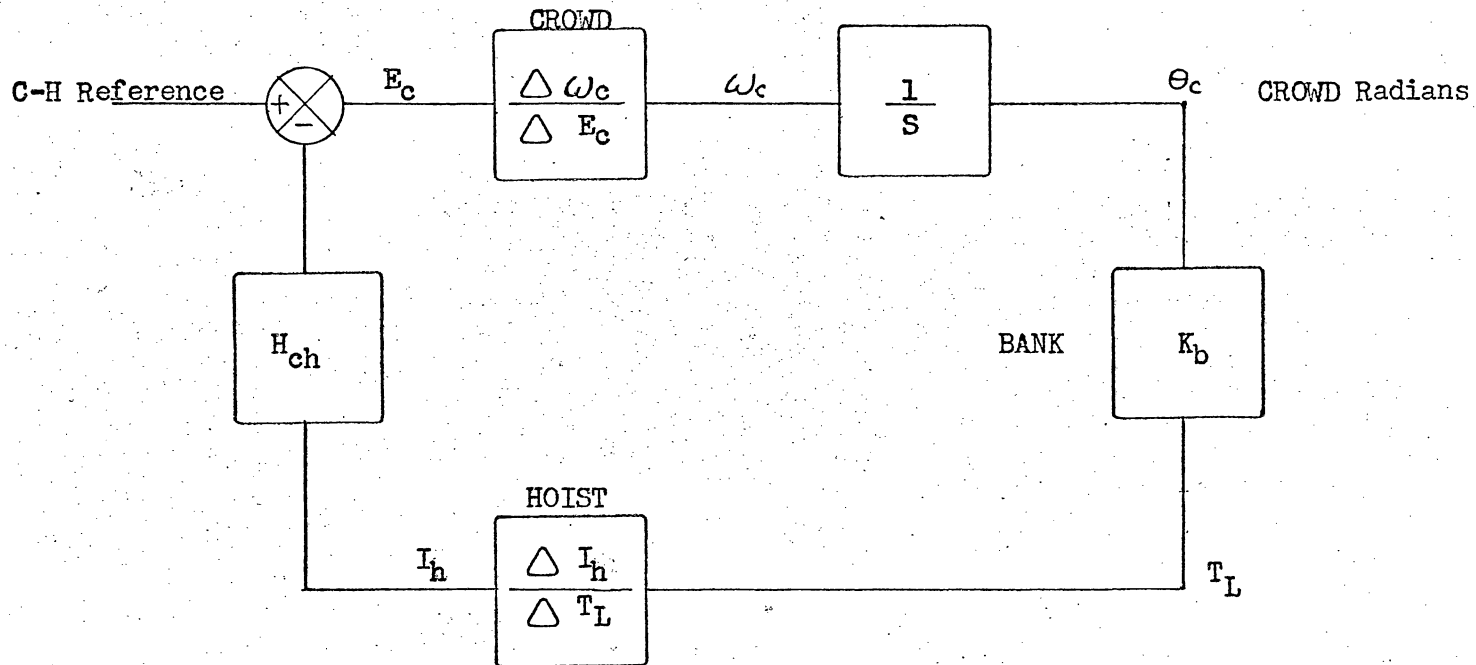


Figure 8. Simplified Model of Crowd-Hoist Regulator

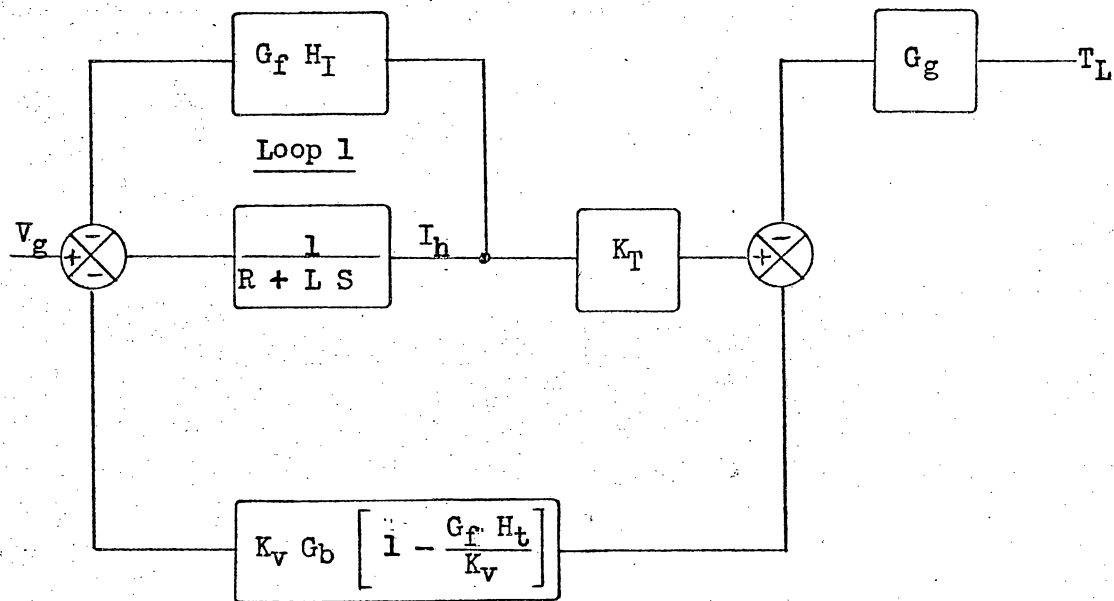
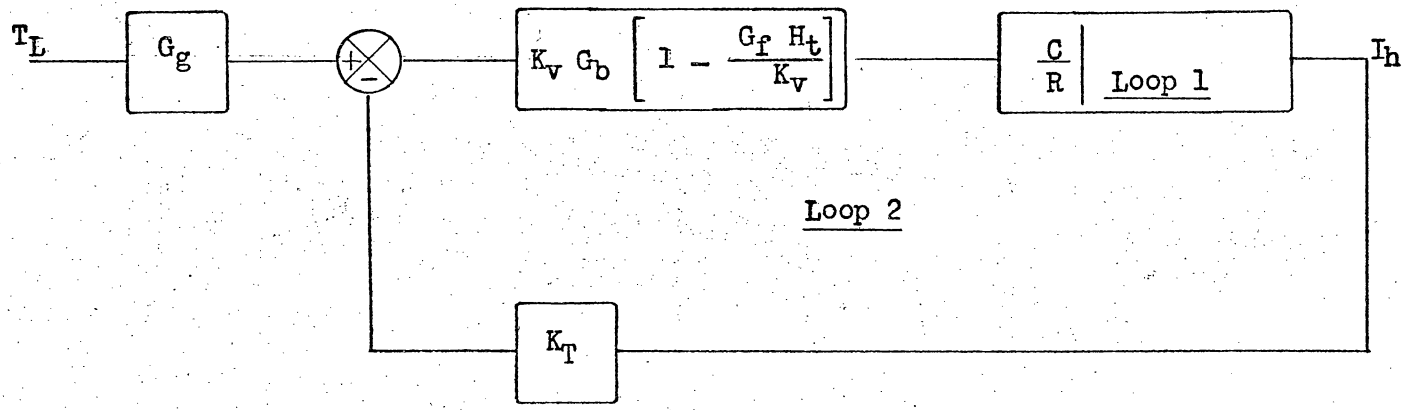


Figure 9. Further Block Reduction of Figure 7



Note: $\frac{\Delta I_h}{\Delta T_L} = G_g \frac{C}{R} \Big|_{\text{Loop 2}}$

Figure 10. Resolution of $\frac{\Delta I_h}{\Delta T_L}$

blocks just described. Therefore the stabilizing influence of H_{ch} will help in obtaining a faster response. The DC gain of H_{ch} will determine directly the change about an operating point in hoist armature current that will be required to drive the crowd motion from its full crowd to full retract position.

Secondly, the H_{ch} element must include a tuned filter to suppress the mechanical oscillatory frequency ω_o which also appears in the hoist armature current signal. This requirement is further stressed by Dr. Black in section P wherein he states that the tuned filter of H_{ch} and the tachometer feedback H_t work together to reduce the magnitude of the mechanical oscillations of the system.

It is intended that the tuned filter in H_{ch} should have the transfer function,

$$H_{TF} = \frac{1 + 2 \zeta_1 T_o S + T_o^2 S^2}{1 + 2 \zeta_2 T_o S + T_o^2 S^2} \quad 4.7$$

where, $\frac{\zeta_1}{\zeta_2} \ll 1$

In concluding this brief summary it should be pointed out that only those sections of immediate interest to this thesis are dwelt on, and of the work reviewed the most important results to be used extensively later in this thesis are equations 4.6 and 4.7, and figure 8.

V. INVESTIGATIONS

A. Development of Motion Transfer Functions

The intent of this section is to develop the required crowd motion and hoist motion transfer functions that are necessary to the analysis of the crowd-hoist regulator system as outlined in section IV.

Figure 11 is a block diagram of the crowd-hoist regulator system and as will be noted, the crowd and hoist motion regulators are tied together through the bank that is being stripped of overburden. The figure 11 is presented to give the reader a vivid appreciation of the magnitude of the problem. Each G and H in this block diagram is a transfer function which in most cases is frequency sensitive (see Appendix 4). In fact, the G_4 block itself represents several cascaded physical gain blocks and is simplified here to gain insight and not lose the reader in trivia.

This section will not concern itself directly with the stability analysis of the crowd and hoist motions as basic voltage regulators with current limit, since this could very easily be a thesis in itself. It is assumed therefore that both motions have been analyzed in detail using any of the many well known techniques of stability analysis. ^(2,3) In practice, as a good first cut at the motion study, a Bode analysis is made using standard Bode techniques. ⁽²⁾ The essential non-linearities of each motion are the saturation of the

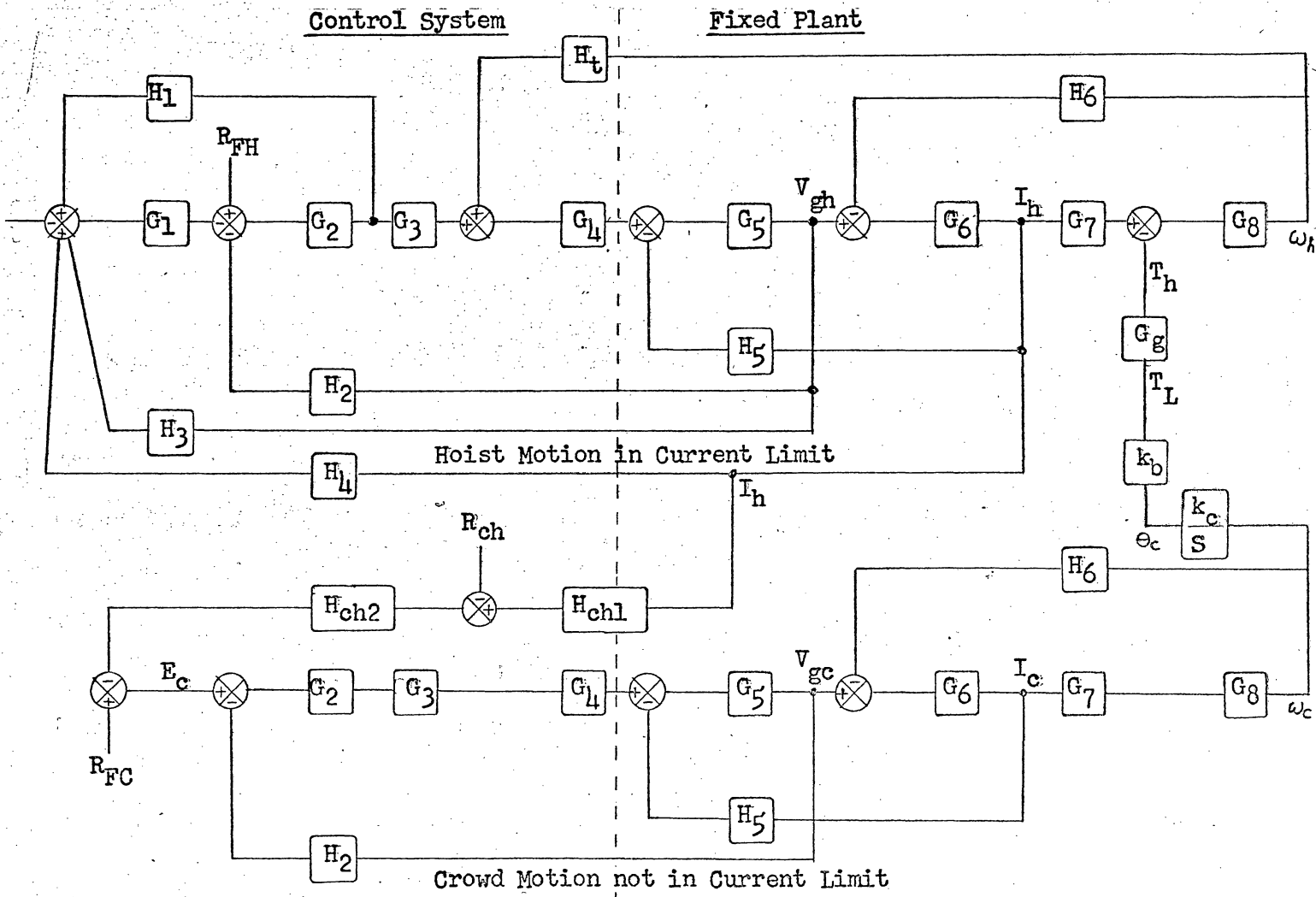


Figure 11. Crowd-Hoist Regulator

generator (G_5) and the generator field exciter (G_4). Since saturation in the forward gain blocks essentially sacrifices performance but does not normally cause instability per se, linear analytical methods are used and a brief discussion of the detrimental effects of the non-linearities will be considered in section VI.

Figure 11 has a dashed line running through about the middle of the page which divides what may be termed the "fixed plant" from the "control system". The fixed plant is merely a term which clearly designates the portion of the system whose transfer functions are fixed in gain and time constants, and is essentially the Ward-Leonard loops of each motion, and of course the entire mechanical system linking the two motions together through the bank.

Section IV outlined the requirements of the crowd-hoist regulator loop in figure 8. From this section it is desired to establish a method to identify the transfer functions $\frac{\omega_c}{E_c}$ and $\frac{I_h}{T_L}$ shown on

figure 8. The H_{ch} feedback network is developed in detail in section VB2.

Also required from this section is a means of determining the transfer function G_f as discussed in section IV and shown on figures 6 and 7. The G_f transfer function is required for the development of the H_t feedback network which is accomplished in section VB1.

The method employed, to resolve the transfer functions required

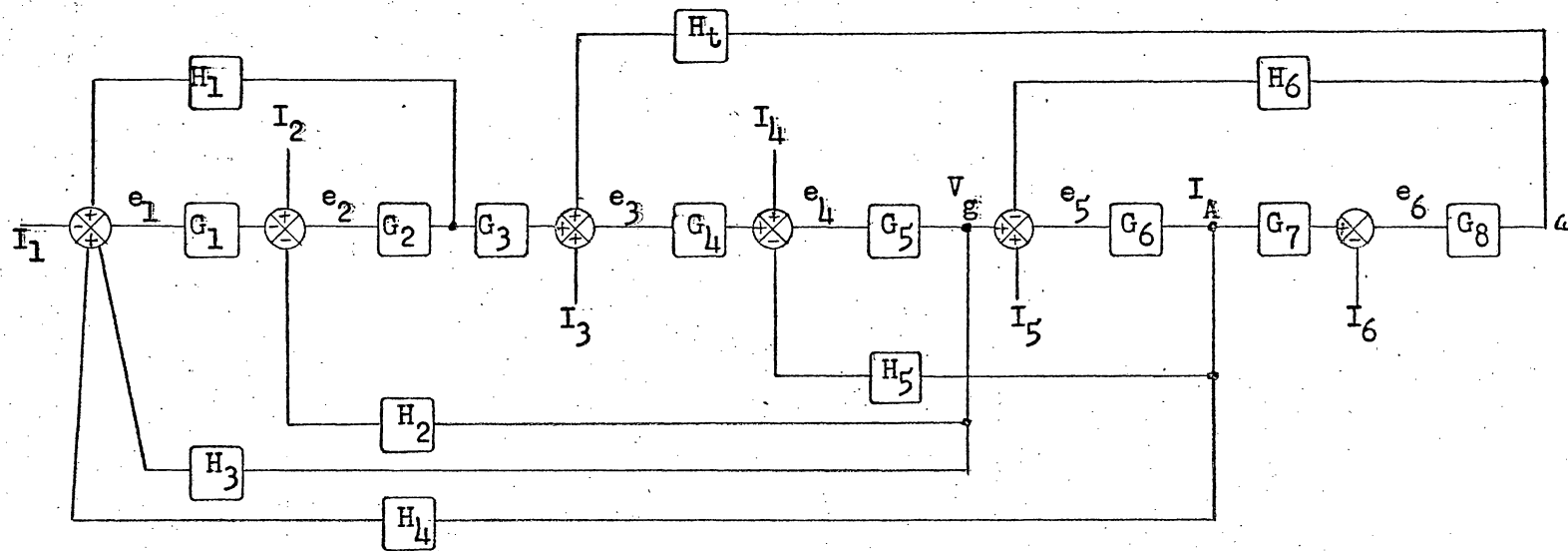


Figure 12. Crowd or Hoist General Block Diagram

for further development of the crowd-hoist regulator system, will be what is termed a determinantal method of resolving transfer functions of a multi-loop feedback system. (3)

Figure 12 shows with generalized block notation the block diagram of the hoist or crowd motions, and this figure is the reference for the derivation of the required transfer functions. Appendix 4 defines more specifically the transfer function content of each of the blocks shown on figure 12 for both the crowd and hoist motions.

The solution of figure 12 for any output point desired as a function of any input (I) can be written in matrix form as follows,

$$\begin{bmatrix} 1 & -G_2H_1 & 0 & -G_5H_3 & -G_6H_4 & 0 \\ G_1 & 1 & 0 & G_5H_2 & 0 & 0 \\ 0 & -G_2G_3 & 1 & 0 & 0 & -G_8H_t \\ 0 & 0 & -G_4 & 1 & G_6H_5 & 0 \\ 0 & 0 & 0 & -G_5 & 1 & G_8H_6 \\ 0 & 0 & 0 & 0 & -G_6G_7 & 1 \end{bmatrix} \begin{bmatrix} e_1 \\ e_2 \\ e_3 \\ e_4 \\ e_5 \\ e_6 \end{bmatrix} = \begin{bmatrix} -I_1 \\ I_2 \\ I_3 \\ I_4 \\ I_5 \\ -I_6 \end{bmatrix}$$

Common to any solution $\frac{e}{I}$ is the denominator or delta of Cramer's rule which is the determinant of the 6 x 6 matrix above. (4) This determinant can be evaluated by continual co-factor reduction until finally it resolved to,

$$\Delta = (1 + G_1 G_2 H_1) \left[1 + G_5 G_6 H_5 + G_6 G_7 G_8 H_6 - G_4 G_5 G_6 G_7 G_8 H_t \right] \\ + G_2 G_3 G_4 G_5 \left[(1 + G_6 G_7 G_8 H_6) (H_2 + G_1 H_3) + G_1 G_6 H_4 \right]$$

This delta will be used in sections VA1, VA2 and VA3 in the derivation of the necessary hoist and crowd motion transfer functions required for this crowd-hoist regulator study.

1. The Hoist Transfer Function G_f

This section derives an expression for the hoist transfer function G_f referred to in Section IV. The G_f hoist motion transfer function is a resolution of the hoist motion considering the input summing junction to be V_R of section IV, figures 6 and 7, and correlates with the I_3 input of figure 12. In accordance with the development in section IV of figures 6 and 7, for this derivation the (I_A) current feedback is neglected, since all current feedback is considered as the H_I transfer function. Also H_t is set equal to zero to agree with the analysis of section IV.

With reference to figure 12, a solution of the matrix development of section VA for $\frac{V_g}{I_3}$ with all other I's equal to zero is given by,

$$\text{since, } V_g = e_4 G_5$$

$$\text{therefore, } \frac{V_g}{I_3} = \frac{e_4}{I_3} G_5$$

The determinant that must be resolved for solution of $\frac{e_4}{I_3}$ is with

$$I_1 = I_2 = I_4 = I_5 = I_6 = 0$$

$$\Delta e_4 = -I_3 \begin{bmatrix} 1 & -G_2 H_1 & 0 & -G_6 H_4 & 0 \\ G_1 & 1 & 0 & 0 & 0 \\ 0 & 0 & -G_4 & G_6 H_5 & 0 \\ 0 & 0 & 0 & 1 & G_8 H_6 \\ 0 & 0 & 0 & -G_6 G_7 & 1 \end{bmatrix}$$

Now with the delta of section VA, the transfer function found by resolving the preceding determinant is,

$$G_f = \frac{V_g}{I_3} = \frac{G_4 G_5}{1 + \frac{G_2 G_3 G_4 G_5 (H_2 + G_1 H_3)}{1 + G_1 G_2 H_1}} \quad 5.2$$

This solution considers $H_t = H_4 = H_5 = 0$

This transfer function can now be evaluated by substituting the particular transfer functions of the hoist motion blocks (Appendix 4) as represented by the G's and H's in the expression for G_f . This will yield an expression of the form,

$$G_f (S) = \frac{N (S)}{D (S)}$$

Then the roots of both N (S) and D (S) may be extracted by means of a digital computer program for resolving the roots of a polynomial. The final expression for G_f will resolve to a major zero, a dominant pair of complex poles, and several other poles which by inspection may be neglected as having only secondary effects on the results.

With this simplification the G_f transfer function is considered to have the form,

$$G_f \approx \frac{k_f (1 + T_f S)}{(1 + bS + aS^2)}$$

which is the form required for use in Appendix 2 in order to continue the analysis of the system H_t feedback network in section VB1.

2. The Hoist Transfer Function $\frac{I_h}{T_h}$

Proceeding with the same methodology as used in the previous section, an expression for the hoist motion transfer function

$\frac{I_h}{T_h}$ is desired which will be used in the stability analysis of the crowd-hoist regulator in section VI.

To obtain $\frac{I_h}{T_h}$ from the matrix development of section VA none of the blocks of figure 12 may be neglected since the hoist is in current limit. However, the only input to consider is I_6 , since the purpose is to look at the effects on hoist armature current I_h caused by torque disturbances at the I_6 input.

Therefore with reference to figure 12, with all I's equal to zero except I_6 ,

$$\frac{I_h}{T_h} = \frac{e_5}{I_6} G_6$$

where, the determinant that must be resolved is,

$$\Delta e_5 = I_6 \begin{vmatrix} 1 & -G_2 H_1 & 0 & -G_5 H_3 & 0 \\ G_1 & 1 & 0 & G_5 H_2 & 0 \\ 0 & -G_2 G_3 & 1 & 0 & -G_8 H_t \\ 0 & 0 & -G_4 & 1 & 0 \\ 0 & 0 & 0 & -G_5 & G_8 H_6 \end{vmatrix}$$

Now with the delta of section VA, the final transfer function is resolved to,

$$\frac{I_h}{T_h} = \frac{N_2}{D_2} \quad 5.2$$

$$N_2 = G_6 G_8 \left[(H_6 - G_4 G_5 H_t) (1 + G_1 G_2 H_1) + G_2 G_3 G_4 G_5 H_6 (H_2 + G_1 H_3) \right] \quad 5.3$$

$$D_2 = (1 + G_1 G_2 H_1) \left[1 + G_5 G_6 H_5 + G_6 G_7 G_8 H_6 - G_4 G_5 G_6 G_7 G_8 H_t \right] + G_2 G_3 G_4 G_5 \left[(1 + G_6 G_7 G_8 H_6) (H_2 + G_1 H_3) + G_1 G_6 H_4 \right] \quad 5.4$$

There are several points worth mentioning in regard to evaluating this transfer function. The hoist transfer function block G_8 of figure 12 is in our analysis the function G_b of equation 4.2 section IV. Also to obtain the transfer function $\frac{I_h}{T_L}$ of figure 8,

it must be noted from figure 5, that the following relationship exists,

$$\frac{I_h}{T_L} = \frac{I_h}{T_h} G_g \quad 5.5$$

where G_g is given by equation 4.3

Also evaluation of equation 5.2, in addition to the hoist motion transfer functions to be found in Appendix 4, requires an expression for the transfer function H_t which is to be found in Appendix 2 equation A2.1.

Otherwise, the evaluation of equation 5.2 in terms of its roots are found by the digital computer program the same as equation 5.1 of section VA1.

3. The Crowd Transfer Function $\frac{\omega_c}{E_c}$

Similar to the last two sections, the matrix development of section VA and figure 12 will be used to resolve the crowd motion transfer function $\frac{\omega_c}{E_c}$.

Since, as shown on figure 11, it is assumed throughout this study that the crowd motion is not in current limit, the G_1 block of figure 12 is set equal to zero. This simulates that G_1 , the current limit amplifier, is in its dead space or zero gain region. The H_t block is also set equal to zero since, it is not part of the crowd motion. The present concern is to resolve the crowd motion and look at the effect on the output of crowd speed which will be caused by the crowd-hoist reference on the crowd error E_c . Therefore with reference to figure 12 with all I's equal to zero except I_2 , the transfer function sought is given by,

$$\frac{\omega_c}{E_c} = \frac{e_6}{I_2} G_8$$

where the determinant that must be resolved is,

$$\Delta e_6 = I_2 \begin{vmatrix} 1 & -G_2 H_1 & 0 & -G_5 H_3 & -G_6 H_4 \\ 0 & -G_2 G_3 & 1 & 0 & 0 \\ 0 & 0 & -G_4 & 1 & G_6 H_5 \\ 0 & 0 & 0 & -G_5 & 1 \\ 0 & 0 & 0 & 0 & -G_6 G_7 \end{vmatrix}$$

Again, with the delta of section VA, the final transfer function becomes,

$$\frac{\omega_c}{E} = \frac{G_2 G_3 G_4 G_5 G_6 G_7 G_8}{G_5 G_6 H_5 + (1 + G_6 G_7 G_8 H_6) (1 + G_2 G_3 G_4 G_5 H_2)} \quad 5.6$$

This transfer function can now be evaluated by substituting the particular crowd motion block transfer functions to be found in Appendix 4 for the G's and H's in equation 5.6.

Then the roots of the polynomials in S are obtained by the digital program as is done in the previous two sections.

This concludes section VA, and the results of this entire section will be required to accomplish the stability analysis of the crowd-hoist regulator in section VI.

B. Development of Crowd-Hoist Circuits

This section will concern itself with the application of figure 8, and equations 4.6 and 4.7 of section IV in order to develop the practical circuitry⁽⁵⁾ needed to fulfill the system requirements of a Crowd-Hoist regulator as outlined previously in section IV.

There are two main developments which are necessary to this section,

- 1) Section VB1 covers the detailed development of the tachometer positive feedback network, H_t by expanding on equation 4.6 and figure 6 of section IV.
- 2) Section VB2 is used to develop in detail the circuitry needed to meet the requirements of the H_{ch} feedback network as presented in section IV. This development draws on figure 8 and equation 4.7 of section IV.

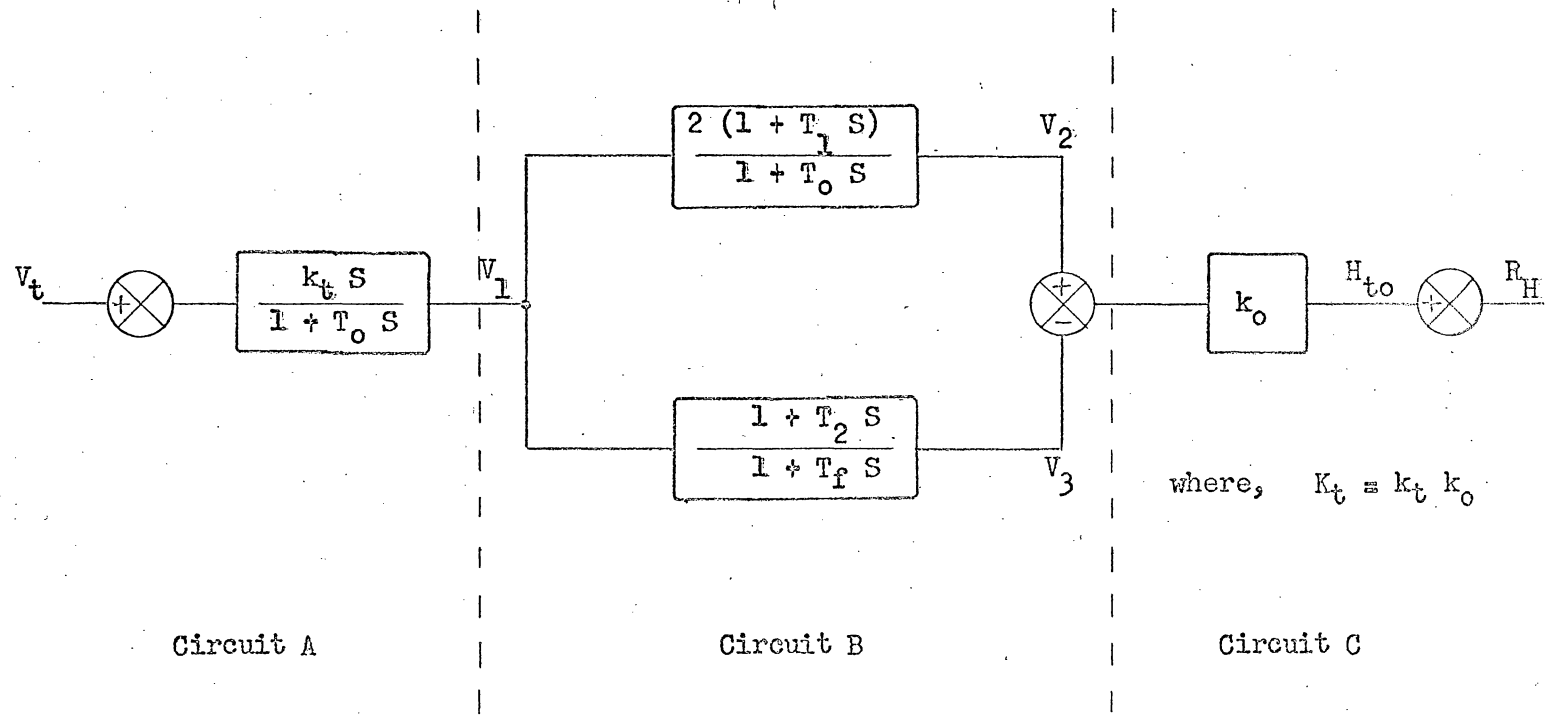
1. H_t Feedback Network

This section is concerned with the application of equation 4.6 for H_t from section IV page 21 as further developed in Appendix 2. Figure 23 of Appendix 2, shows a general block diagram for H_t (S).

From this beginning it is desired to develop general operational amplifier circuitry which will be able to perform this function. The standard operational amplifier which will be used is operated from ± 50 volt DC buses, and has a saturation level of ± 30 volt with a 10 ma load, and has the high gain, approximately 10^5 , required of an operational amplifier. Obviously, to apply linear analysis⁽⁶⁾ means that the operational amplifiers must not be driven into their respective saturation region by their respective signal input levels at any time.

From figure 23 of Appendix 2, the primary concern is the development of the circuitry for the transfer function $\frac{H_{to}}{V_t}$. The gain block K_m, which has the transfer function $\frac{V_t}{\omega_m}$, includes the gain from hoist motor output shaft (ω_m), through gearing and the voltage gain of the tachometer itself. The voltage output of the tachometer is defined throughout this analysis as V_t.

Figure 13 is the block diagram for $\frac{H_{to}}{V_t}$ in accordance with Appendix 2 and figure 23. It is the intention of this section to



where, $K_t = k_t k_o$

Figure 13. H_t Feedback Network $\frac{\Delta H_{to}}{\Delta V_t}$

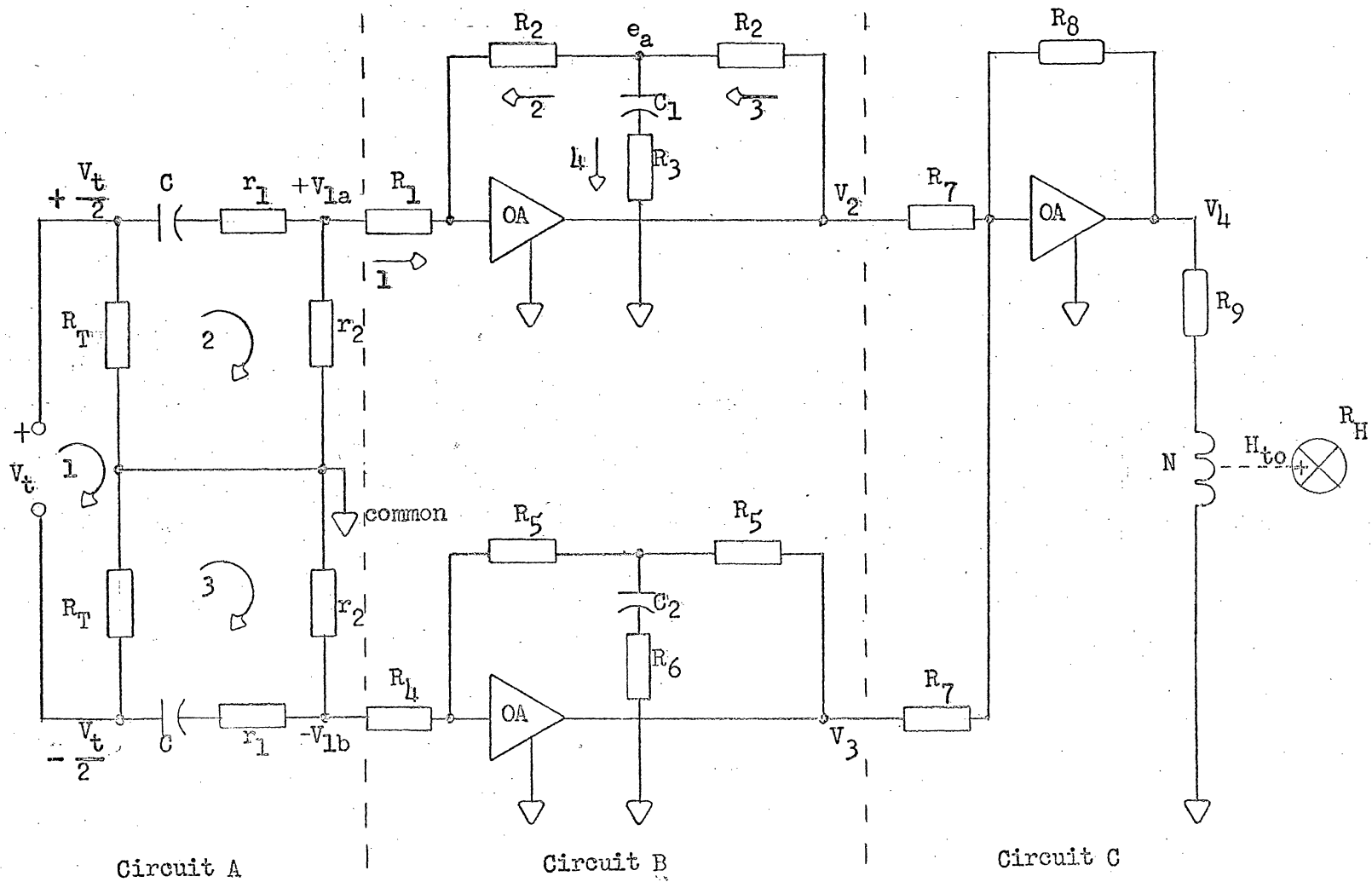


Figure 14. H_t Feedback Circuits

establish that the operational circuit schematic of figure 14 will meet the requirements of figure 13. To accomplish this equivalence consider the circuit of figure 14 in the three cross-referenced sections of figures 13 and 14.

Circuit A is the input circuit for tach output voltage, and as such it has, per se, a large potential signal to noise ratio. This is especially true since the circuit is basically a differentiator with a series capacitance input. The physical fact that the tachometer, located at the hoist motor, is about 100 feet from the control panel, which will contain the H_t feedback network, adds to the potential input noise generation. These factors must be considered when wiring of such circuitry is done on the job site.

An expression for the gain block $\frac{V_1}{V_t}$ may be obtained by applying Kirchhoff's loop equations⁽⁷⁾ to the three loops forming circuit A and assuming that R_1 and R_4 are much greater than r_2 .

The three loop equations obtained are,

$$\begin{aligned}
 2R_T i_1 & & - R_T i_2 & & - R_T i_3 & & = V_t \\
 - R_T i_1 & + \left[R_T + r_1 + r_2 + \frac{1}{CS} \right] i_2 & & & & & = 0 \\
 - R_T i_1 & & & + \left[R_T + r_1 + r_2 + \frac{1}{CS} \right] i_3 & & & = 0
 \end{aligned}$$

The solution by determinants for i_2 is,

$$i_2 = \frac{V_t}{2} \frac{CS}{[1 + (r_1 + r_2)CS]}$$

For the point V_{1a} on figure 14,

$$V_{1a} = i_2 r_2$$

Therefore,

$$V_{1a} = \frac{V_t}{2} \frac{r_2 C S}{[1 + (r_1 + r_2) C S]}$$

Because of the circuit symmetry the point V_{1b} on figure 14 is,

$$V_{1b} = - \frac{V_t}{2} \frac{r_2 C S}{[1 + (r_1 + r_2) C S]} = - V_{1a}$$

Therefore for either point the gain block $\frac{V_1}{V_t}$ is,

$$\frac{V_1}{V_t} = \frac{r_2 C S}{2 [1 + (r_1 + r_2) C S]} = \frac{k_t S}{1 + T_o S} \quad 5.7$$

By bridging the tach input and centering $2 R_T$, an operational amplifier is saved which would otherwise be required for sign inversion. Therefore, the input signal sign inversion at the input of circuit B on figure 14 serves the same purpose as the summing junction at the input of circuit C on figure 13, as regards polarity of signals V_2 and V_3 .

As mentioned earlier, the signal to noise ratio could be a problem in the field when the control system is installed. It is always wise for the systems circuit designer to bear this in mind and allow alternatives accordingly. In this case, a problem of high frequency noise could be minimized by providing a pole in the transfer function $\frac{V_1}{V_t}$, which would act to suppress high frequency noise and yet not be detrimental to the system bandwidth.

Such a pole in $\frac{V_1}{V_t}$ could be provided by paralleling resistor r_2 with a capacitor C_2 . If this action were taken the transfer function would be modified as follows,

$$r_2 \text{ becomes, } Z_2 = \frac{r_2}{1 + r_2 C_2 S}$$

and,

$$\frac{V_1}{V_t} = \frac{r_2 C S}{2 \{1 + [(r_1 + r_2) C + r_2 C_2] S + r_1 r_2 C C_2 S^2\}}$$

and for this case,

$$\text{let } a = r_1 r_2 C C_2$$

$$b = (r_1 + r_2) C + r_2 C_2$$

then,

$$T_o = \frac{b + \sqrt{b^2 - 4a}}{2}$$

and the added pole is,

$$T = \frac{b - \sqrt{b^2 - 4a}}{2}$$

Now, assuming the problem is high frequency noise that is that, $T_0 \geq 20 T$ very little effect on T_0 itself has occurred.

Circuit B is the next cross-referenced section of figures 13 and 14 to be considered. Both of the branches shown will utilize passive elements in conjunction with an operational amplifier. For such a configuration, the transfer function is easiest to derive by means of nodal equations based again on Kirchhoff's law. (8) Using the basic assumption of a virtual ground (9) at the summing junction of the operational amplifier, the following nodal equations for the top branch of circuit B on figure 14 may be written,

$$i_1 = \frac{V_{1a}}{R_1} \quad i_2 = \frac{e_a}{R_2} \quad i_3 = \frac{V_2 - e_a}{R_2} \quad i_4 = \frac{e_a}{R_3 + \frac{1}{C_1 S}}$$

at the summing junction,

$$i_1 + i_2 = 0$$

at point e_a ,

$$i_3 = i_2 + i_4$$

Simultaneous solution of these equations yields,

$$\frac{V_2}{V_{1a}} = - \frac{2 R_2}{R_1} \left[\frac{1 + (R_3 + \frac{R_2}{2}) C_1 S}{1 + R_3 C_1 S} \right] \quad 5.8$$

By analogy, the lower branch of circuit B in figure 14 is,

$$\frac{V_3}{V_{1b}} = -2 \frac{R_5}{R_4} \left[\frac{1 + (R_6 + 2) C_2 S}{1 + R_6 C_2 S} \right] \quad 5.9$$

The minus sign merely agrees with the sign inversion of an operational amplifier. Based on the assumption of Appendix 3 that,

$$T_2 > T_f \quad \text{and} \quad T_1 > T_o$$

this configuration will serve its purpose.

Circuit C is an operational amplifier used for straight DC gain, and its transfer function by inspection is,

$$\frac{V_4}{V_2} = \frac{V_4}{V_3} = - \frac{R_8}{R_7}$$

Now the signals injected at the hoist motion summing junction labeled R_H on figure 14 are a function of the current and field turns of their respective control fields. In other words, the device next following the summing junction R_H is a magnetic amplifier in the hoist motion which has multiple input, isolated control fields and whose gain is expressed in terms of volts out versus ampere turns excitation. Consequently, the excitation applied to the summing junction R_H by signal H_{to} is simply with reference to figure 14,

$$H_{to} = V_4 \frac{N}{R_9}$$

where, N = number of turns in the H_{to} control field

$$\frac{V_4}{R_9} = \text{amperes through the } H_{to} \text{ control field}$$

therefore, $\frac{H_{to}}{V_4} = \frac{N}{R_9}$

and, for the gain block k_o of figure 13 we have,

$$k_o = \frac{H_{to}}{V_2} = \frac{H_{to}}{V_3} = -\frac{R_8}{R_7} \frac{N}{R_9} \quad 5.10$$

Now, since throughout this section linear circuit operation is assumed, the superposition theorem⁽⁶⁾ holds and for positive V_{1a} , H_{to} will be positive and conversely for negative V_{1b} , H_{to} will be negative, all with respect to the center-tapped common.

In the final circuit design, the fact of linear operation must be shown in accordance with Appendix 3.

A summary of the results of this section in terms of correlating figures 13, 14 and 23 as regards the transfer function $\frac{H_{to}}{V_t}$ is

as follows,

$$K_t = k_t k_o$$

For circuit A from equation 5.7,

$$k_t = \frac{r_2 C}{2} \quad 5.11$$

$$T_o = (r_1 + r_2) C \quad 5.12$$

For circuit B from equations 5.8 and 5.9,

$$\frac{R_2}{R_1} = 1 \quad 5.13$$

$$T_1 = \left[R_3 + \frac{R_2}{2} \right] C_1 \quad 5.14$$

$$T_o = R_3 C_1 \quad 5.15$$

$$\frac{R_5}{R_4} = \frac{1}{2} \quad 5.16$$

$$T_2 = \left[R_6 + \frac{R_5}{2} \right] C_2 \quad 5.17$$

$$T_f = R_6 C_2 \quad 5.18$$

The prime interest is in gain magnitude from circuit C equation 5.10 and therefore,

$$k_o = \frac{R_8}{R_7} \frac{N}{R_9} \quad 5.19$$

$$\text{and, } K_t = k_t k_o = \frac{r_2 C R_8 N}{2 R_7 R_9} \quad 5.20$$

This concludes section VB1. The results above, equations 5.11 through 5.20, will be required for calculation of all circuit components in the H_t feedback circuit when values are assigned to the system parameters K_t , T_o , T_f , a and b of appendix 2.

2. The H_{ch} Feedback Network

a. Defining The H_{ch} Network

This section is concerned primarily with the H_{ch} block of figure 8, section IV, page 23. It is appropriate at this time to redraw figure 8 in a more detailed fashion in order to develop the H_{ch} feedback network in a logical manner. Figure 15 is figure 8 redrawn in order to more clearly emphasize the important characteristics which the H_{ch} feedback network must have.

Figure 15 defines the $H_{ch}(S)$ feedback network as the transfer function from I_h (hoist armature current) to E_c (crowd error). This was established in section IV as the essential function of $H_{ch}(S)$. Figure 16, page 53 shows the $H_{ch}(S)$ network redrawn from figure 15, and it is figure 16 that will be developed in detail in this section.

However, before proceeding to figure 16, there are several points that deserve expression at this time in order to allow a better understanding later of how and why figure 15 will fulfill the requirements of an automatic crowd-hoist regulator.

The general operation of the knee -action shovel during the dipper loading cycle is explained in the introduction to this thesis (section III), and figure 1, page 8 and familiarity with its basic operation is imperative here.

First, it is anticipated that the automatic crowd-hoist regulator will be a supplementary function. The normal operation of

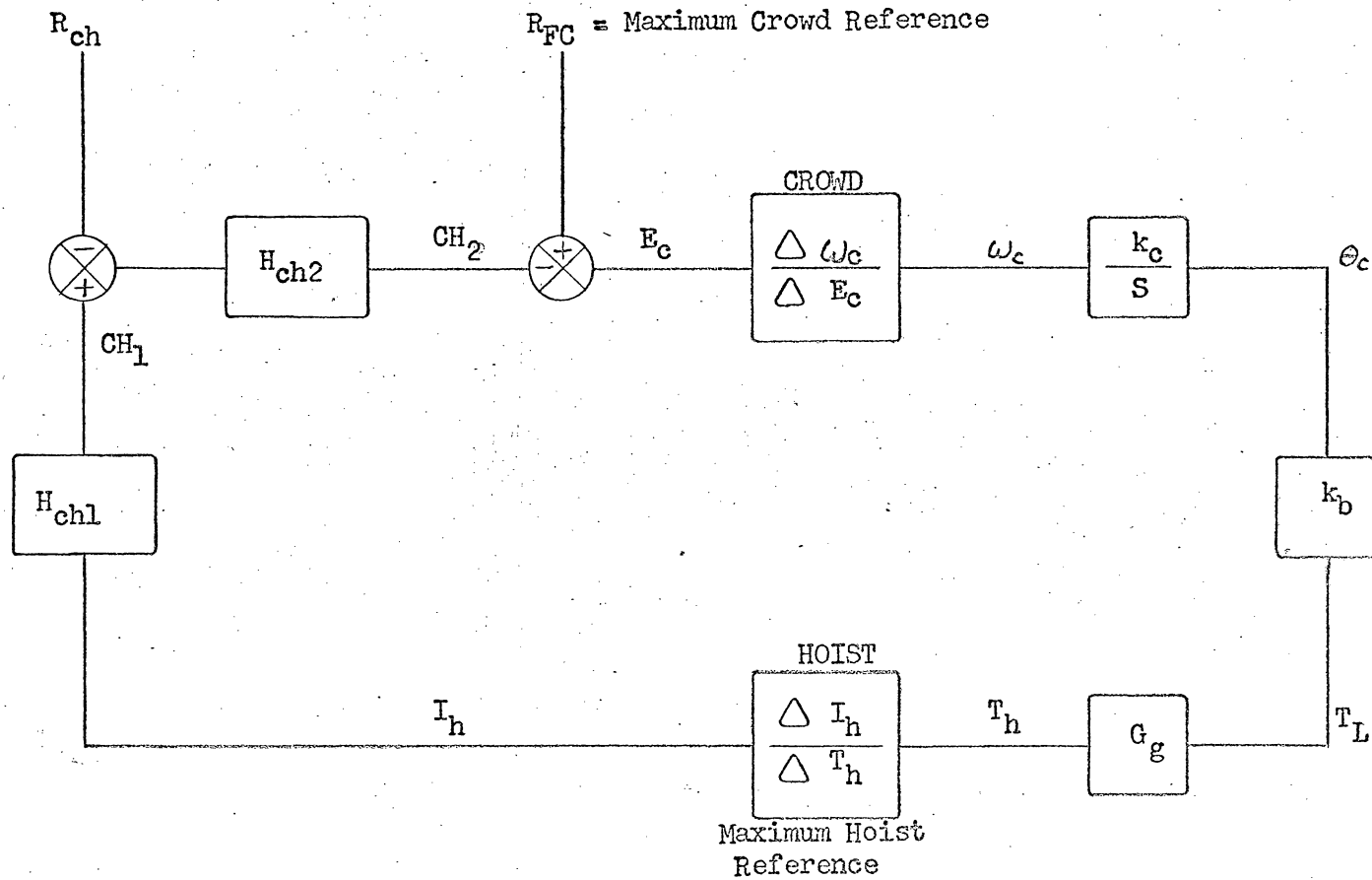


Figure 15. Model of Crowd-Hoist Regulator

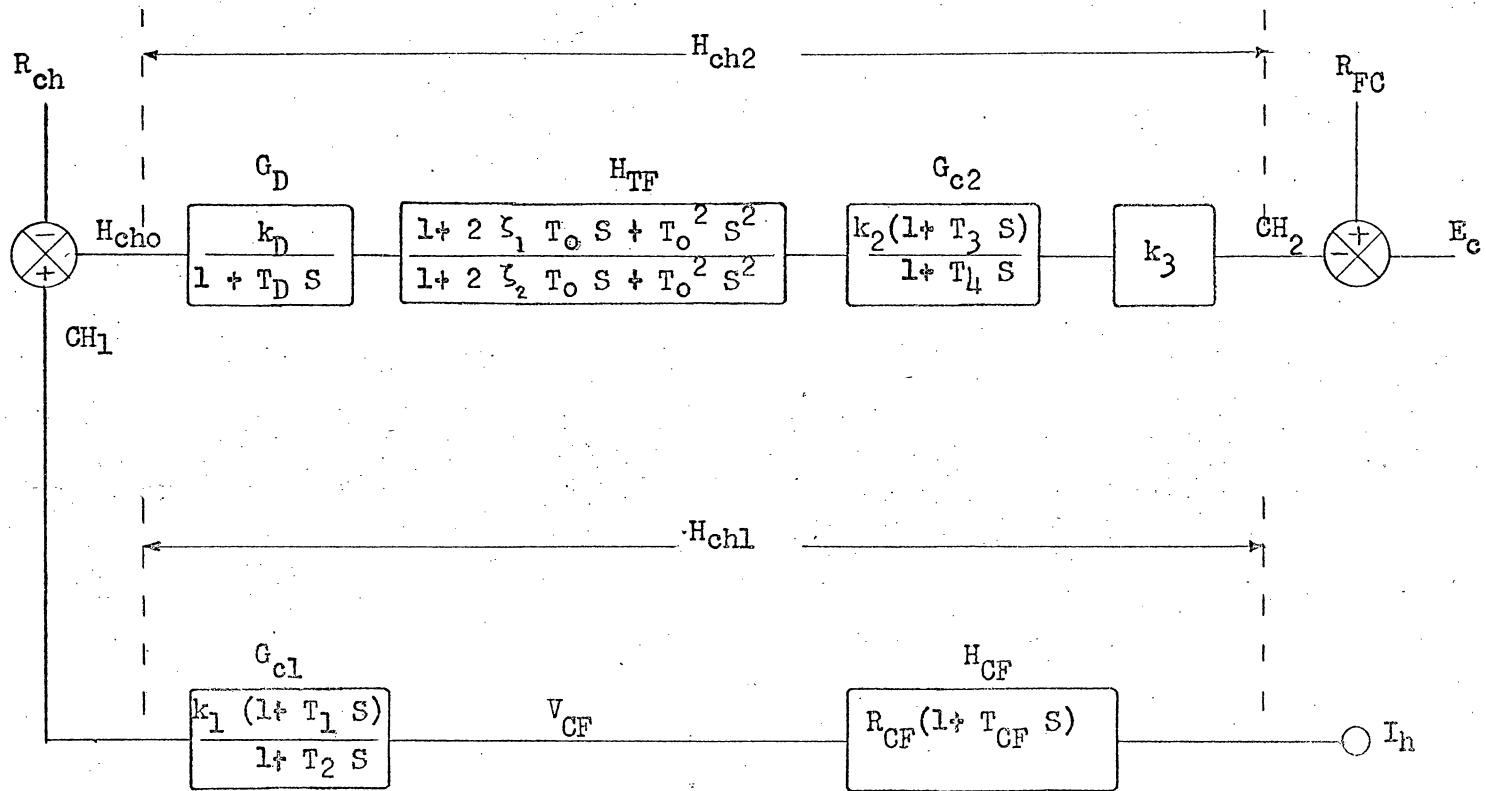


Figure 16. H_{ch} Feedback Network $\frac{\Delta E_c}{\Delta I_h}$

a stripping shovel is under the manual control of a highly skilled operator to all times. This operator at present accomplishes the dipper loading cycle by acting as the feedback element $H_{ch}(S)$. He does this by simply watching the dipper as it moves into and up through the bank. If the dipper begins to gain speed and come out of the bank, he moves his crowd master switch in the "crowd" direction thus forcing the dipper into the bank. Conversely if the dipper, in describing its natural constant hoisting arc, is shoved too deeply into the bank, the hoist motion will stall out on its current limit characteristic. To counteract this the operator moves his crowd master switch in the "retract" direction, and this serves to unload the hoist motion sufficiently to allow the dipper loading cycle to continue. In other words, the operator presently accomplishes the crowd-hoist regulator function by watching the dipper's hoisting motion, and crowding or retracting, with the crowd motion, whichever action in his judgment is called for at any instant. This further establishes the shovel operator requirements of manual dexterity and visual acuity first mentioned in the introduction.

Of course, the basic desire of engineering is to try to optimize any iterative process by making it automatic. In the present case, it is felt that the optimum dipper loading cycle can be realized by holding the hoist motion in the first quadrant on the current limit slope of its volt-ampere characteristic as shown in

figure 3, page 11. This says that the desire is to fully utilize the capability of the machinery in its most efficient manner, and the current limit action is there to protect the machinery from abuse. Therefore, the operational goal of the automatic crowd-hoist regulator is to select a value of hoist armature current (I_{ho}) on the current limit slope of the hoist motion, and automatically crowd or retract the crowd motion in order to hold this value of I_{ho} throughout the dipper loading cycle.

However, for safety reasons, it is desired that the shovel operator be able to regain manual control at his discretion. It is for this reason that the biasing effects of R_{ch} and R_{EC} are required as shown on figure 15, and these effects will be discussed now. The present operational concept of the automatic crowd-hoist regulator as envisioned by Mr. M. Neslin⁽¹⁾, and incorporating what has been outlined above, is as follows.

The shovel operator will begin the dipper loading cycle by bringing the dipper in low to the ground towards the foot of the bank. When the dipper is approximately in the position shown in figure 1, page 8, the operator will move both the hoist and crowd master switches into a position not normally used in manual operation. The placing of both master switches in these respective positions will initiate the automatic crowd-hoist regulator and its reference R_{ch} . At the same instant, and by the same action, the hoist motion will be given maximum hoist reference signal R_{FH} , and the maximum

crowd reference signal R_{FC} will be given to the crowd motion.

The act of starting both motions in maximum reference to begin the automatic dipper loading operation, immediately forces the hoist motion on to its current limit slope. The action of the crowd-hoist regulator, operating on the crowd error, holds the dipper into the bank, throughout the dipper loading cycle without stalling the hoist motion.

The automatic crowd-hoist reference R_{ch} determines the value of hoist armature current (I_{ho}) which the crowd-hoist regulator will endeavor to maintain. This is what the $H_{ch}(S)$ feedback network must accomplish, and these requirements may now be expressed mathematically with reference to figure 15 and figure 16.

First, an expression for the crowd error E_c as a function of the hoist armature current I_h is from Figure 15,

$$E_c = R_{FC} - CH_2 \quad 5.21$$

$$\text{where, } CH_2 = \left[I_h H_{ch1} - R_{ch} \right] H_{ch2} \quad 5.22$$

Now defining an operating point on the hoist motion current limit slope as follows,

$$\text{when, } I_h = I_{ho} \quad E_c = 0$$

$$\text{therefore, } CH_2 = -R_{FC}$$

This states that when the hoist armature current attains the instantaneous value (I_{ho}), zero error on the crowd motion will occur at that instant, and the crowd motion should neither crowd nor retract.

The open loop gain, that is, the crowd-hoist regulator system GH of figure 15, will dictate the maximum excursions of hoist armature current which the system will allow. These allowable perturbations, about the operating point I_{ho} may be written as $\pm \Delta I_{ho}$.

By differentiating equation 5.21 and 5.22 with respect to I_h , and considering everything else constant as it would be for the steady state case, then equations 5.21 and 5.22 show that,

$$d E_c = -H_{ch1} H_{ch2} dI_h$$

or,

$$\frac{\Delta E_c}{\Delta I_h} = -H_{ch1} H_{ch2} = -H_{ch}$$

This result agrees with the physical picture by stating that for increasing I_h , decreasing E_c is desired. In other words, as the dipper moves deeper into the bank, causing the hoist motion to slow down, the hoist armature current increases. When this happens, the crowd motion is to move in the retract direction, and this requires that E_c decrease. Conversely for decreasing I_h increasing E_c is evident.

Therefore, placing an operating constraint on E_c and CH_2 as follows,

$$R_{FC} \text{ (Full Retract)} \leq E_c \leq R_{FC} \text{ (Full Crowd)}$$

$$-2R_{FC} \leq CH_2 \leq 0$$

From this analysis, the following three mathematical relationships ensue,

$$\begin{aligned} \text{for } I_h &= I_{ho} & E_c &= 0 \\ \left[I_{ho} \quad H_{chl} \quad - R_{ch} \right] H_{ch2} &= R_{FC} \end{aligned} \quad 5.23$$

$$\begin{aligned} \text{for } I_h &= I_{ho} + \Delta I_{ho} & E_c &= - R_{FC} \\ \left[(I_{ho} + \Delta I_{ho}) \quad H_{chl} \quad - R_{ch} \right] H_{ch2} &= 2 R_{FC} \end{aligned} \quad 5.24$$

$$\begin{aligned} \text{for } I_h &= I_{ho} - \Delta I_{ho} & E_c &= R_{FC} \\ \left[(I_{ho} - \Delta I_{ho}) \quad H_{chl} \quad - R_{ch} \right] H_{ch2} &= 0 \end{aligned} \quad 5.25$$

R_{FC} is fixed by the crowd motion regulator and represents full crowd reference for that regulator, and $- R_{FC}$ is full retract reference for the crowd motion. Therefore, the magnitude of R_{FC} is a constant defined by the requirements of the crowd motion regulator. The magnitude of the perturbation ΔI_{ho} is defined as follows,

$$\left| \Delta I_{ho} \right| = a I_{ho}$$

Since the interest at this time is to consider only steady state operating conditions, DC gain of H_{ch2} will be held constant and a solution to equations 5.24 and 5.25 based on these constraints is desired.

Then equation 5.24 becomes,

$$(1 + a) I_{ho} H_{ch1} - R_{ch} = \frac{2R_{FC}}{H_{ch2}}$$

and equation 5.25 becomes,

$$(1 - a) I_{ho} H_{ch1} - R_{ch} = 0$$

Simultaneous solution of these equations for H_{ch1} and R_{ch} yields,

$$H_{ch1} = \frac{R_{FC}}{a I_{ho} H_{ch2}} \quad 5.26$$

$$R_{ch} = \frac{(1 - a) R_{FC}}{a H_{ch2}} \quad 5.27$$

$$\text{where } a = \frac{|\Delta I_{ho}|}{I_{ho}} \quad 5.28$$

These three basic equations will determine the steady state gain requirements of the entire H_{ch} feedback network and the prime concern now is a more detailed consideration of figure 16.

b. Development Of H_{ch1} and H_{ch2}

Section VB2a was a general development of the H_{ch} feedback network in terms of steady state gain requirements, defining the crowd-hoist regulator operating point I_{ho} and the biasing effects of R_{FC} and R_{ch} .

This section will cover the particular development of the circuitry which will make up the transfer functions $H_{ch1}(S)$ and $H_{ch2}(S)$ as shown on figure 15, page 52 and in greater detail on figure 16, page 53 .

Figure 16 defines the general form of the several transfer function blocks which combine to form the main blocks $H_{ch1}(S)$ and $H_{ch2}(S)$. Each will be dealt with separately.

The transfer function $H_{ch1}(S)$, as can be seen from figure 16, consists of two blocks and the circuitry to be used to generate these transfer functions are cross-referenced with figure 17.

The H_{CF} block is part of the fixed plant and represents the commutating field voltage drop V_{CF} as a function of the hoist armature current I_h . The transfer function can be calculated simply as,

$$V_{CF} = I_h \left[R_{CF} + L_{CF} S \right]$$

$$\text{where, } R_{CF} = R_{HMCF} + R_{HGCF}$$

$$L_{CF} = L_{HMCF} + L_{HGCF}$$

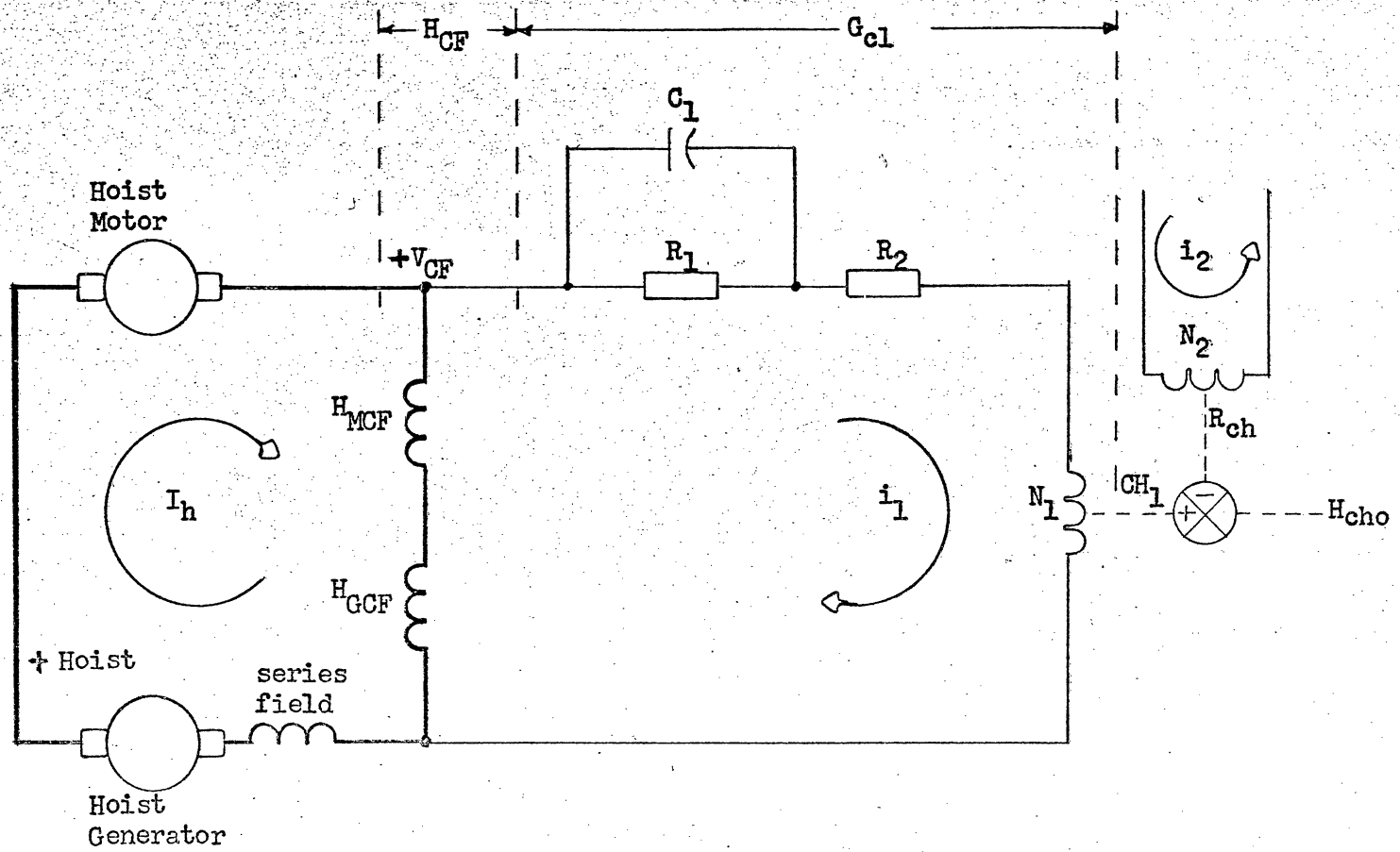


Figure 17. H_{chl} Feedback Circuit $\frac{\Delta CH_1}{\Delta I_h}$

yielding,

$$H_{CF} = \frac{V_{CF}}{I_h} = R_{CF} \left[1 + T_{CF} S \right] \quad 5.29$$

$$\text{where, } T_{CF} = \frac{L_{CF}}{R_{CF}}$$

The commutating field voltage drop signal V_{CF} is proportional to the I_h armature current signal, and in addition offers the additional advantage of an inherent lead signal in the transfer function as can be seen. This lead signal has been found to be very beneficial at times in the Bode analysis of a system because it inherently increases the phase margin.

The G_{C1} block of figures 16, page 53, and 17 has two functions. It must provide a means of controlling the gain of the H_{ch1} network, and allow another lead signal which can compensate other predominate lags inherent in the system.

The dotted lines on figure 17 identify the summing junction of the signals CH_1 and R_{ch} as inputs to the magnetic amplifier represented by block G_D on figure 16 and 18. Therefore, continuing the derivation of the G_{C1} block, an expression for the current i_1 through the control field N_1 is desired,

$$i_1 = \frac{V_{CF}}{Z_1 + R_2}$$

$$\text{where, } Z_1 = \frac{R_1}{1 + R_1 C_1 S}$$

Consequently, the signal CH_1 applied at the summing junction in terms of control field excitation of G_D is,

$$\frac{i_1 N_1}{V_{CF}} = \frac{N_1}{R_1 + R_2} \left[\frac{1 + R_1 C_1 S}{1 + \frac{R_1 R_2 C_1 S}{R_1 + R_2}} \right] \quad 5,30$$

This result identifies the G_{C1} block transfer function as,

$$k_1 = \frac{N_1}{R_1 + R_2} \quad 5,31$$

$$T_1 = R_1 C_1 \quad 5,32$$

$$T_2 = \frac{R_1 R_2 C_1}{R_1 + R_2} \quad 5,33$$

The signal R_{ch} , which will be used to establish the operating point I_{ho} of the crowd-hoist regulator, is introduced at the summing junction of G_D in a manner analogous to the signal CH_1 .

The concern now is the circuit development of the transfer function H_{ch2} which is made up of the cascaded blocks shown on figure 16, page 53 and cross-referenced with figure 18.

The lead element G_D , is a magnetic amplifier which, as mentioned earlier, has multiple input, isolated control fields. The gain k_D of G_D is expressed in terms of volts output versus ampere turns excitation of its multiple control fields. The time

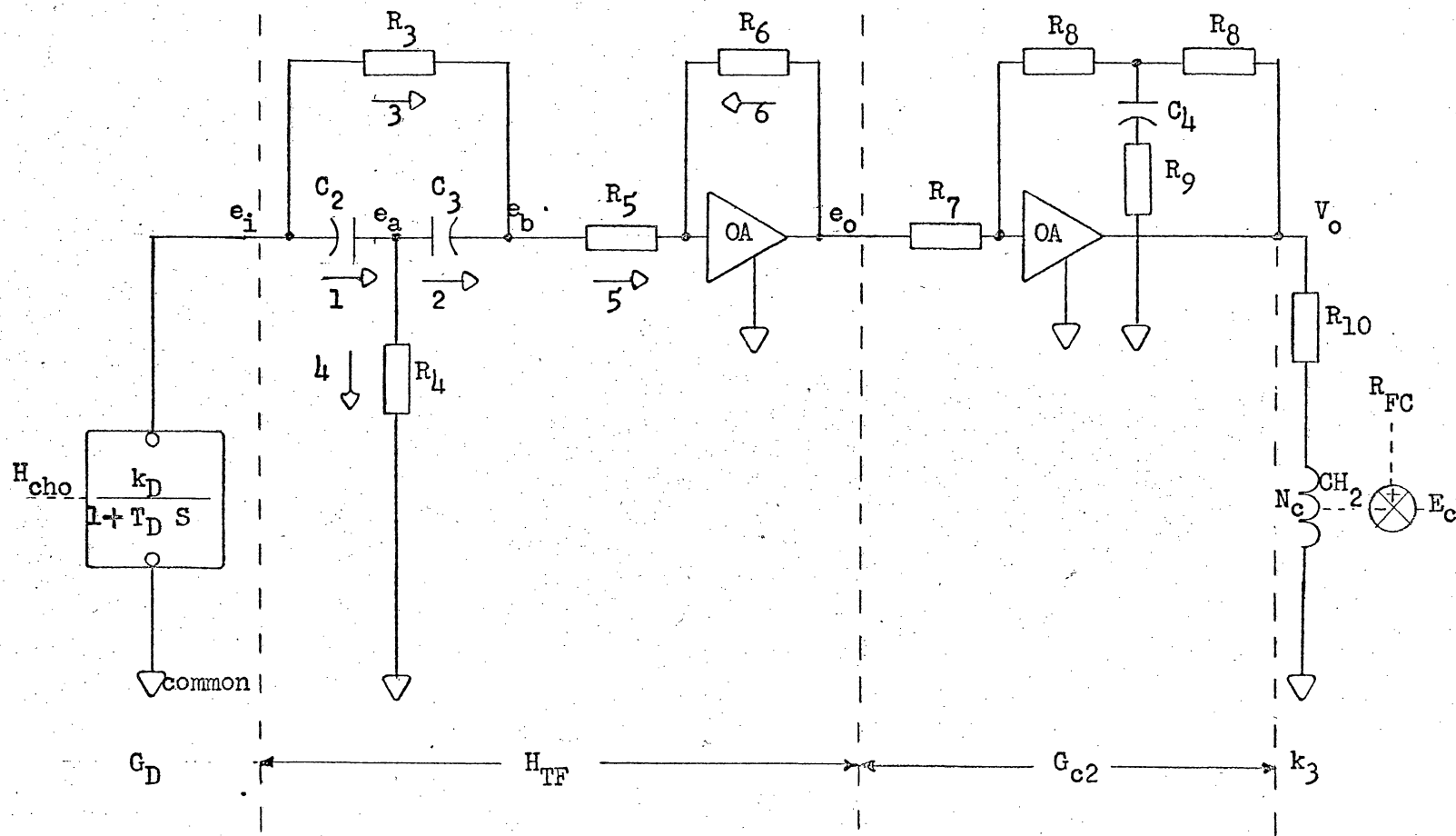


Figure 18. H_{ch2} Feedback Circuit

$$\frac{\Delta CH_2}{\Delta H_{cho}}$$

constant T_D of G_D is the summation of all of the $\frac{L}{R}$'s of its respective control fields. In this case the magnetic amplifier G_D has as its power source a built in inverter power supply of frequency 2.5 KC. Due to the high frequency of its power source and the very low inductance of its control fields, the time constant T_D is of the order of 10^{-3} , and for the purpose, can be considered negligible in comparison with the inherent system time constants. The purpose of G_D in this circuit is to obtain electrical isolation from the Ward-Leonard loop and provide the gain k_D .

The next transfer function which is cross-referenced on figure 16, page 53, and 18 is H_{TF} . The purpose of the tuned filter H_{TF} is to provide a means of eliminating the system mechanical oscillatory frequency ω_0 which the hoist armature current signal I_h is expected to contain. The H_{TF} requirement is discussed in section IV and in particular, evolves around the use of equation 4.7. It should be noted that the transfer function of the H_{TF} block is identical to equation 4.7.

The H_{TF} operational circuit of figure 18, will now be derived using the basic assumption of a virtual ground at the summing junction of the operational amplifier and the same nodal techniques as was employed in section VB1.

$$\begin{aligned}
 i_1 &= (e_i - e_a) C_2 S & i_4 &= \frac{e_a}{R_4} \\
 i_2 &= (e_a - e_b) C_3 S & i_5 &= \frac{e_b}{R_5} \\
 i_3 &= \frac{(e_i - e_b)}{R_3} & i_6 &= \frac{e_o}{R_6}
 \end{aligned}$$

The three basic Kirchoff's equations that must be satisfied are,

$$i_1 = i_2 + i_4$$

$$i_2 + i_3 = i_5$$

$$i_5 + i_6 = 0$$

The simultaneous solution of the equations yields,

$$\frac{-e_o}{e_i} = \frac{R_6}{R_3 + R_5} \left[\frac{R_3 R_4 C_2 C_3 S^2 + R_4 (C_2 + C_3) S + 1}{R_p R_4 C_2 C_3 S^2 + [R_4 (C_2 + C_3) + R_p C_3] S + 1} \right]$$

where, $R_p = \frac{R_3 R_5}{R_3 + R_5}$

Under the condition that, $R_5 \gg R_3$ $R_p \rightarrow R_3$

and the following identities relate the H_{TF} circuit of figure 18 and the H_{TF} block transfer function (equation 4.4) of figure 16, page 53.

$$\frac{R_6}{R_3 + R_5} = 1 \quad 5.34$$

$$R_3 R_4 C_2 C_3 = T_o^2 \quad 5.35$$

$$R_4 (C_2 + C_3) = 2 \zeta_1 T_o \quad 5.36$$

$$R_4 (C_2 + C_3) + R_p C_3 = 2 \zeta_2 T_o \quad 5.37$$

Since the ratio of $\frac{\zeta_1}{\zeta_2} \geq \frac{1}{10}$

$$R_p C_3 \leq R_4 (C_2 + C_3) \quad 5.38$$

The ratio of $\frac{\zeta_1}{\zeta_2}$ determines the depth of the notch, and T_o is

inversely proportional to the frequency ω_0 at which the notch will be centered on the frequency response curve.

Since the system mechanical oscillatory frequency is of the order of 1 cps, there were many problems encountered in deriving an operational circuit which would meet the analytical requirements of equation 4.7. For example, it is a desired property of H_{TF} that the parameter T_o be variable without effecting the parameter ζ_1 and vice versa. This property can be demonstrated by considering equations 5.36 and 5.37, and the following expression derived from

the basic relationships 5.35 through 5.37,

$$\frac{\zeta_1}{\zeta_2} = \frac{1+r}{1+r} \left(1 + \frac{R_3}{R_4}\right) \quad 5.39$$

$$\text{where, } r = \frac{C_3}{C_2} \quad 5.40$$

Now, by using ganged rheostats for R_3 and R_4 and varying them directly such that the ratio $\frac{R_3}{R_4}$ remains constant, the parameter T_0 can be varied without effecting ζ_1 .

The operational circuit represented as G_{c2} on figures 16, page 53, and 18 has precisely the same form as the "B" operational circuits of the H_t feedback network in section VB1. Therefore the analogous solution for G_{c2} from this earlier work can be written directly.

Here again, as with the G_{c1} transfer function, the desire is to introduce another potential lead signal into the overall system transfer function.

$$G_{c2} = - \frac{2 R_8}{R_7} \left[\frac{1 + (R_9 + \frac{R_8}{2}) C_4 S}{1 + R_9 C_4 S} \right] \quad 5.41$$

In terms of correlating the G_{c2} block transfer function of figure 16

with our operational circuit of figure 18 the resulting equations are,

$$k_2 = - \frac{2 R_8}{R_7} \quad 5.42$$

$$T_3 = (R_9 + \frac{R_8}{2}) C_4 \quad 5.43$$

$$T_4 = R_9 C_4 \quad 5.44$$

The last element of H_{ch2} is the block identified as k_3 on figure 16, page 53. Here also an analogy with the transfer function $\frac{H_{to}}{V_4}$ of section VB1 exists so that k_3 can be written by inspection

$$\text{as, } k_3 = \frac{CH_2}{V_o} = \frac{N_c}{R_{10}} \quad 5.45$$

Again it should be noted that the signal CH_2 is introduced into the crowd error by means of a magnetic amplifier which is the lead element in the crowd motion.

This concludes section VB2b. The results of this section, namely equations 5.29 through 5.45, will be required for calculation of all the circuit components in the H_{ch} feedback network along with equations 5.21 through 5.28 of section VB2a when values are assigned to the other system parameters T_o , I_{ho} , ΔI_{ho} and the system transfer functions $\frac{\omega_c}{E_c}$ and $\frac{I_h}{T_h}$.

VI. DISCUSSION OF RESULTS

A. Summary of Procedures

This thesis is essentially a presentation of the design criteria which were developed to meet the analytical requirements of an automatic crowd-hoist regulator as outlined in section IV. It, therefore, seems appropriate to begin this section by summarizing the methods and procedures necessary to the utilization of the generalized equations of section V. It should be borne in mind continually that there are two goals,

1. The H_t feedback network and tuned filter in the H_{ch2} feedback network have been designed to suppress the fundamental mechanical system oscillatory frequency ω_0 .
2. The blocks of the simplified model of the crowd-hoist regulator, figure 15, page 52, must be quantitatively identified in order to allow an analysis of the closed loop response and stability of the crowd-hoist regulator.

Based on these two prime considerations, a logical procedure is as follows,

1. Observations of the mechanical system⁽¹⁾ and appendix 1.
 - a) The system inertias J_M and J_L must be found from knowledge of the shovel geometry and the overburden being stripped.
 - b) With the dipper in the air, a torque impulse disturbance

is introduced into the mechanical system, From recordings of the response to this impulse it is possible to get a reasonable approximation for the mechanical oscillatory frequency ω_0 .

- c) Using this value of ω_0 , equation 4.1 defines the spring torsion constant K_r .
- d) Knowing K_r and correlating the well documented time response curves for second order systems⁽²⁾ with the recordings taken earlier, allows identification of the mechanical system damping constant. This yields a good approximation to the $2 \zeta_1 T_o$ term of equation 4.7 and direct correlation with the $\frac{D}{K_r}$ of equation 4.4.
- e) Thus $J_M, J_L, \omega_0, T_o, K_r, D$ and ζ_1 are identified.

2. Calculation of the H_t feedback network.

- a) Section VA1 will yield an expression for the hoist motion transfer function G_f , which will identify the system parameters T_f, a, b and k_f .
- b) With a knowledge of T_f, a, b and k_f from section VA1, ζ_1 and T_o from system analysis of section IV and appendix 1, and, K_V and K_M from appendix 2, the H_t network parameters K_t, T_1 and T_2 can be evaluated.
- c) Now section VB1 allows direct evaluation of all the H_t network circuit parameters shown in figure 14,

page 43, by using equations 5.11 through 5.20.

- d) Appendix 3 is then used to verify linearity of the H_t feedback network as designed.
 - e) This completes the design of the H_t feedback network for the system parameters found earlier.
3. The H_{ch} DC gains and R_{ch} reference from Section VB2a
- a) From the hoist motion settings for the current limit characteristic as shown on figure 3, page 11 an operating point I_{ho} , for the automatic dipper loading cycle is determined based on observations of hoist generator voltage and armature current obtained while the shovel operator performs a manual dipper loading cycle.
 - b) The perturbation of hoist armature current, ΔI_{ho} is also selected empirically from the observations above.
 - c) From the crowd motion regulator, the parameter R_{FC} is known and is simply the amount of reference (ampere turns) required to drive the crowd motion into "full crowd". Since the crowd motion is a voltage regulator, "full crowd" means the application of maximum crowd generator voltage to the crowd motor.
 - d) With this information, section VB2a allows the DC gains of H_{ch1} and H_{ch2} to be set and establishes a value for the automatic crowd-hoist regulator reference R_{ch} by utilizing equations 5.21 through 5.28.

4. Calculation of the H_{ch1} and H_{ch2} feedback networks from Section VB2b.
 - a) From the hoist motion, the transfer function H_{CF} of figure 17, page 61, is defined.
 - b) The G_{c1} block of figure 17, page 61, and the G_{c2} block of figure 18, page 64, are both intended as series compensation by providing potential lead signals to cancel the inherent secondary system time constants in $\frac{\omega_c}{E_c}$ and $\frac{I_h}{T_h}$.
 - c) The tuned filter H_{TF} of H_{ch2} figure 18 is intended to suppress or damp the systems basic mechanical oscillatory frequency which is present in the hoist armature current signal I_h , by essentially cancelling the systems natural second order response. $(T_o^2 s^2 + 2 \zeta_1 T_o s + 1)$, and replacing it with a dominant pair of complex poles with a larger damping constant $(T_o^2 s^2 + 2 \zeta_2 T_o s + 1)$.
 - d) Thus section VB2b allows calculation of the entire H_{ch} feedback network by proper use of equations 5.29 through 5.45.
5. Identification of the crowd-hoist regulator loop blocks of figure 15, page 52.
 - a) From section VA3 by using appendix 4, the crowd motion

transfer function $\frac{\omega_c}{E_c}$ is evaluated.

- b) Similarly, section VA2 allows quantitative identification of the hoist motion transfer function $\frac{I_h}{T_h}$.
- c) The function G_g is given by equation 4.3 and figure 5, page 17, and evaluated by using the previously found values of D , K_r and J_L .
- d) The transfer function k_c requires direct knowledge of the crowd motion mechanical gearing ratios in order to determine the change in crowd position θ_c as a function of crowd speed ω_c .
- e) As stated earlier the H_{ch1} and H_{ch2} functions making up the H_{ch} feedback network are evaluated by utilizing sections VB2a and VB2b.
- f) k_b , as stated in section IV, is taken as a straight gain term whose magnitude is not easily determined. This obstacle however is not insurmountable as the analysis in the second part of this section will show.

This concludes a summary of the methods and procedures established by section V, and it should be noted that the two goals stated at the beginning of this section have been satisfied with this approach.

In the next part of section VI, Bode techniques will be employed to analyze the closed loop stability of the crowd-hoist regulator model of figure 15 page 52.

B, Bode Analysis of System GH

Utilizing the results of section V and the methods and procedures of section VI A, it is now possible to analyze the closed loop stability of the crowd-hoist regulator model of figure 15, page 52.

Figure 15 identifies the system GH as,

$$GH(S) = H_{ch2} \frac{\omega_c}{E_c} \frac{k_c}{S} k_b G_g \frac{I_h}{T_h} H_{chl} \quad 6.1$$

Since the system is defined as a function of S, any of the standard techniques of linear analysis⁽²⁾ could be applied at this point.

Whatever technique is employed the basic concept remains the same.

The basic concept is, as always, the search for the roots of the characteristic equation,

$$1 + GH(S) = 0$$

The Root Locus technique⁽²⁾ accomplishes this solution by mapping the locus of all points on the S plane which will satisfy the condition,

$$GH(S) = -1$$

that is,

$$|GH(S)| = 1$$

$$\angle GH(S) = -180^\circ$$

The Bode technique⁽²⁾ lets S equal $j\omega$ and considers a frequency domain solution of the same characteristic equation by plotting separately $|GH(j\omega)|$ versus the angular frequency ω , and $\angle GH(j\omega)$

versus angular frequency. Visual inspection of both plots yields the gain, $|GH(j\omega)|$, and the phase angle, $\angle GH(j\omega)$, for any angular frequency. Again, the point of absolute stability is where,

$$|GH(j\omega)| = 1$$

$$\angle GH(j\omega) = -180^\circ$$

Therefore, using Bode techniques, the angular frequency ω_{co} , which is defined as the "crossover" angular frequency of the system, defines the critical point of interest where,

$$|GH(j\omega)| = 1$$

Then from the plot of $\angle GH(j\omega)$ is obtained the phase angle of the function $GH(j\omega)$ at the same angular frequency ω_{co} . If the condition exists such that, $\angle GH(j\omega) = -180^\circ$ at ω_{co} an oscillator of angular frequency ω_{co} in the time domain has been created. The other classic example is where the following condition exists,

$$\angle GH(j\omega) = -90^\circ \quad \text{at } \omega_{co}$$

This case will have essentially the response characteristics of a single time constant system which has the usual physical properties of a simple exponential rate of rise and decay in the time domain.

Any practical real-world system is expected to fall somewhere within this range and the difference between the $\angle GH(j\omega)$ and 180° is termed the phase margin of the system. Therefore, the phase margin (θ) is generally defined as,

$$\theta = 180^\circ + \angle GH(j\omega)$$

For industrial control systems, it is generally considered good design practice to maintain a phase margin of about 40° which means,

$$\angle GH(j\omega) \approx 140^\circ$$

To make Bode Analysis an easier tool, it is common practice to use a Bode ruler with a phase angle scale.⁽²⁾ This feature eliminates the requirement for plotting $\angle GH(j\omega)$ versus ω , by allowing the phase angle $\angle GH(j\omega)$ to be read from the gain versus ω plot of the straight line approximation for $|GH(j\omega)|$.

Since Bode analysis techniques will be used for the study of the system $GH(S)$, the intention of this section so far has been to cite only the very basic concept of Bode's approach to the solution of the classic characteristic equation. It is assumed that the reader has a fluent knowledge of the standard Bode analysis techniques.

Now it is desirable to return to equation 6.1 and figure 15, page 52 for the prime purpose of demonstrating the use of the two compensation transfer functions, G_{c1} and G_{c2} , in the H_{ch} feedback network.

In order to better understand the compensation techniques to be used, it is best that the GH equation 6.1 and figure 15 be understood as consisting of two main sections as follows,

$$\frac{I_h}{E_c} = \frac{\omega}{E_c} \frac{k_c}{S} k_b G_g \frac{I_h}{T_h} \quad 6.2$$

and,

$$\frac{E_c}{I_h} = H_{ch} = H_{ch1} H_{ch2}$$

therefore, from section VB2a figure 16, page 53,

$$\frac{E_c}{I_h} = H_{CF} G_{c1} G_D H_{TF} G_{c2} k_3 \quad 6.3$$

this of course means that equation 6.1 may be rewritten as,

$$GH(S) = \frac{I_h}{E_c}(S) \frac{E_c}{I_h}(S) \quad 6.4$$

Furthermore, from equation 5.26 of section VB2a the DC gain term of H_{ch} is given by,

$$H_{ch} = \left| \frac{R_{FC}}{\Delta I_{ho}} \right| \quad 6.5$$

There are also two simplifying assumptions which will allow direct access to the important aspects of equation 6.3,

- 1) The time constant T_D of G_D is at least 20 times smaller than the next smaller H_{ch} time constant. Therefore, the effects of T_D are negligible to the system GH.
- 2) The H_{TF} tuned filter, as pointed out in section VI A, is the ratio of two second order polynomials of different damping constants. The complex zeros (damping constant ζ_1) are intended to cancel the complex poles (also of damping constant ζ_1) which are expected to appear in the signal from hoist armature current (I_h). Now assuming

H_{TF} is properly tuned, the cancellation is assumed to be effective and the Bode analysis of the system GH will only consider the denominator of H_{TF} .

This means equation 6.3 may be expressed as,

$$\frac{E_c}{I_h} = \frac{R_{FC}}{I_h} \frac{(1 + T_{CF} S) G_c(S)}{(1 + 2 \zeta_2 T_o S + T_o^2 S^2)} \quad 6.6$$

where $G_c(S)$ is an expression which includes only the time constant of $G_{c1} G_{c2}$ from figure 16, page 53 as follows,

$$G_c(S) = \frac{1 + T_1 S}{1 + T_2 S} \frac{1 + T_3 S}{1 + T_4 S} \quad 6.7$$

Now equation 6.2 may be reconsidered in order to gain insight and also to simplify it for the coming Bode analysis. The following two points are worth considering,

- 1) By putting in a step at E_c of figure 15, page 52, with the CH_2 signal temporarily disconnected, and monitoring the output quantity I_h , it is possible to get an approximation to the gain term of $\frac{I_h}{E_c}$. This gain term will be the

rate of integration due to the $\frac{1}{S}$ of $\frac{I_h}{E_c}$. Since everything

in $\frac{I_h}{E_c}$ except $\frac{k_c}{S}$ and k_b , has been defined quantitatively,

an approximation of the gain in terms of $\frac{I_h}{E_c}$ will allow

approximation of the terms k_c and k_b .

- 2) Since the complex zero pair of H_{TF} has been neglected, the complex pole pair of $\frac{I_h}{T_L}$ due to the mechanical system,

when it is resolved from section VA3, must also be neglected.

Now a Bode analysis of the system $GH(S)$ as expressed by equation 6.4 and shown in figure 15 will proceed. Since it will add measurably to the insight obtainable from this analysis, the transfer functions making up the system $GH(S)$ will be defined quantitatively. The numbers used will be representative of the actual system, although it should be remembered that the techniques utilized are of greater significance than the numbers themselves.

$$\text{Let, } \frac{\omega_c}{E_c} \approx \frac{250}{\left[1 + 2(.5)(.09)s + (.09)^2 s^2\right] \left[1 + 2(.8)(.03)s + (.03)^2 s^2\right]}$$

Let,

$$\frac{I_h}{T_L} \approx \frac{0.2 \left[1 + 2(.6)(.8)s + (.8)^2 s^2\right]}{(1 + 2s)(1 + s)(1 + .025s) \left[1 + 2(.4)(.015)s + (.015)^2 s^2\right]}$$

Based on a mechanical system $T_o \approx 0.14$

and equation 6.6,

$$\text{Let, } \frac{E_c}{I_h} = \frac{R_{FC}}{\Delta I_{ho}} \frac{(1 + 0.06s) G_c(s)}{\left[1 + 2 \zeta_2 (.14)s + (.14)^2 s^2\right]}$$

Since the complex quadratics given cannot be plotted directly on a Bode with straight line approximations, a method must be employed to properly represent them. Consider the general quadratic,

$$1 + 2 \zeta T S + T^2 S^2$$

there are the usual three possibilities,

1) If $\zeta > 1$ the quadratic is easily factored into two real roots

2) If $\zeta = 1$ the result of factoring is two real and equal roots namely,

$$(1 + TS)^2$$

3) If $\zeta < 1$ the roots are imaginary. However, there are many standard graphs which allow both gain and phase shift correction as a function of the parameter ζ . (2)

Therefore, the complex quadratic can be expressed for a straight line Bode analysis if the intelligence of the damping constant is maintained. This will be done by using the following notation,

$$1 + 2 \zeta TS + T^2 S^2 = \left[\begin{array}{c} 1 + TS \\ (\zeta) \end{array} \right]^2$$

Applying this notation and combining the transfer functions to form GH(S) yields,

$$GH(S) = K_{CH} \frac{(0,6) \left[1 + 0,8S \right]^2 (1 + 0,06S)}{S (1 + 2S)(1 + S) \left[1 + 0,14S \right]^2 \left[1 + .09S \right]^2 \left[1 + .03S \right]^2} \times \frac{G_c(S)}{(1 + .025S) \left[1 + .015S \right]^2} \quad 6.8$$

(ζ_2) (0.5) (0.8)
 (0.4)

where,

$$K_{CH} = 50 \left[\frac{R_{FC}}{\Delta I_{ho}} \right] k_c k_b$$

and, $G_c(S)$ represents the compensating time constants of $G_{c1} G_{c2}$ in the form of equation 6.7.

Figure 19 is the straight line Bode representations of the system $|GH(j\omega)|$ under three conditions as follows,

- 1) Curve A is the Bode for $|GH(j\omega)|$ of equation 6.8 with,

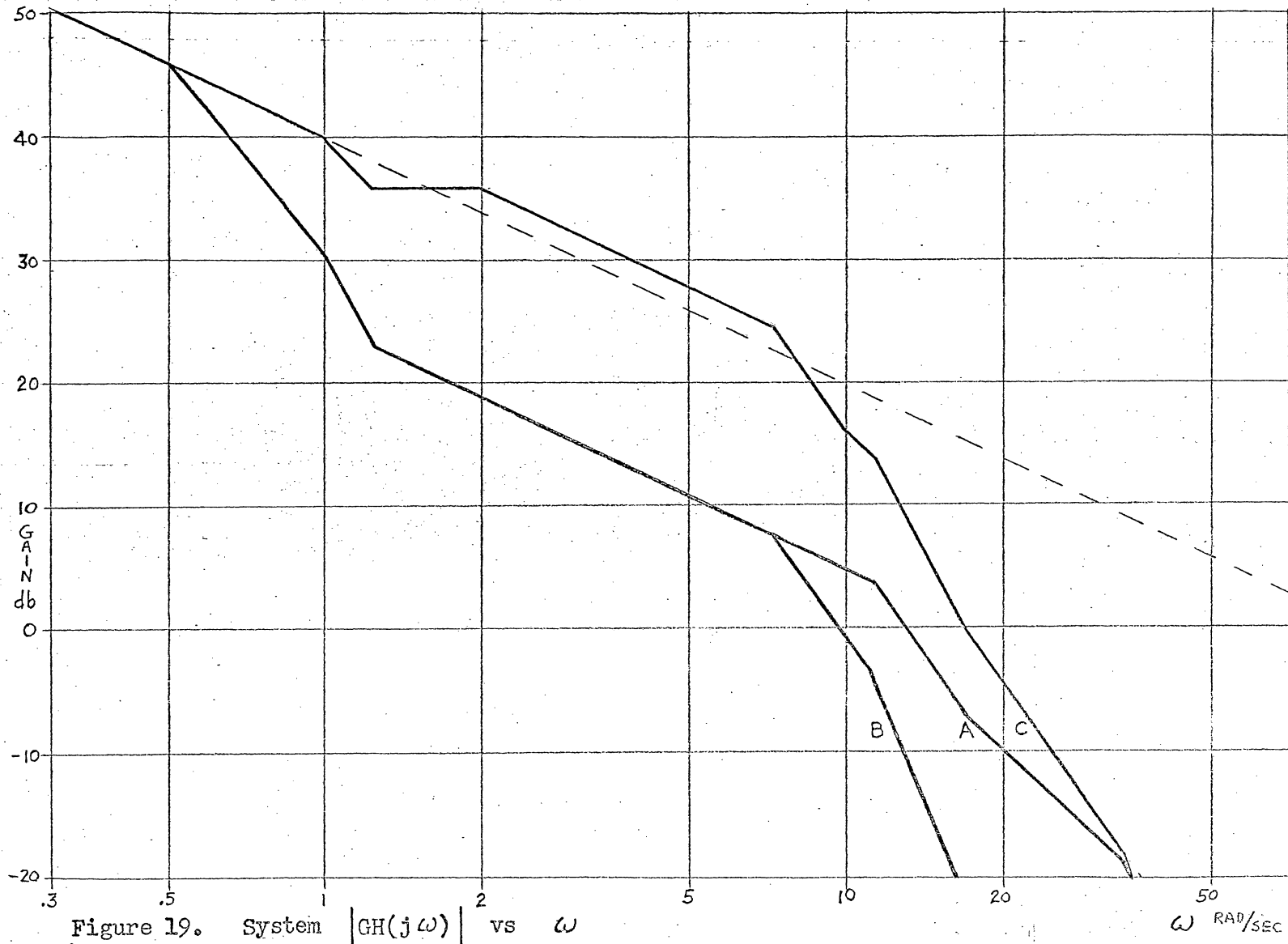
$$G_c(S) = 1$$

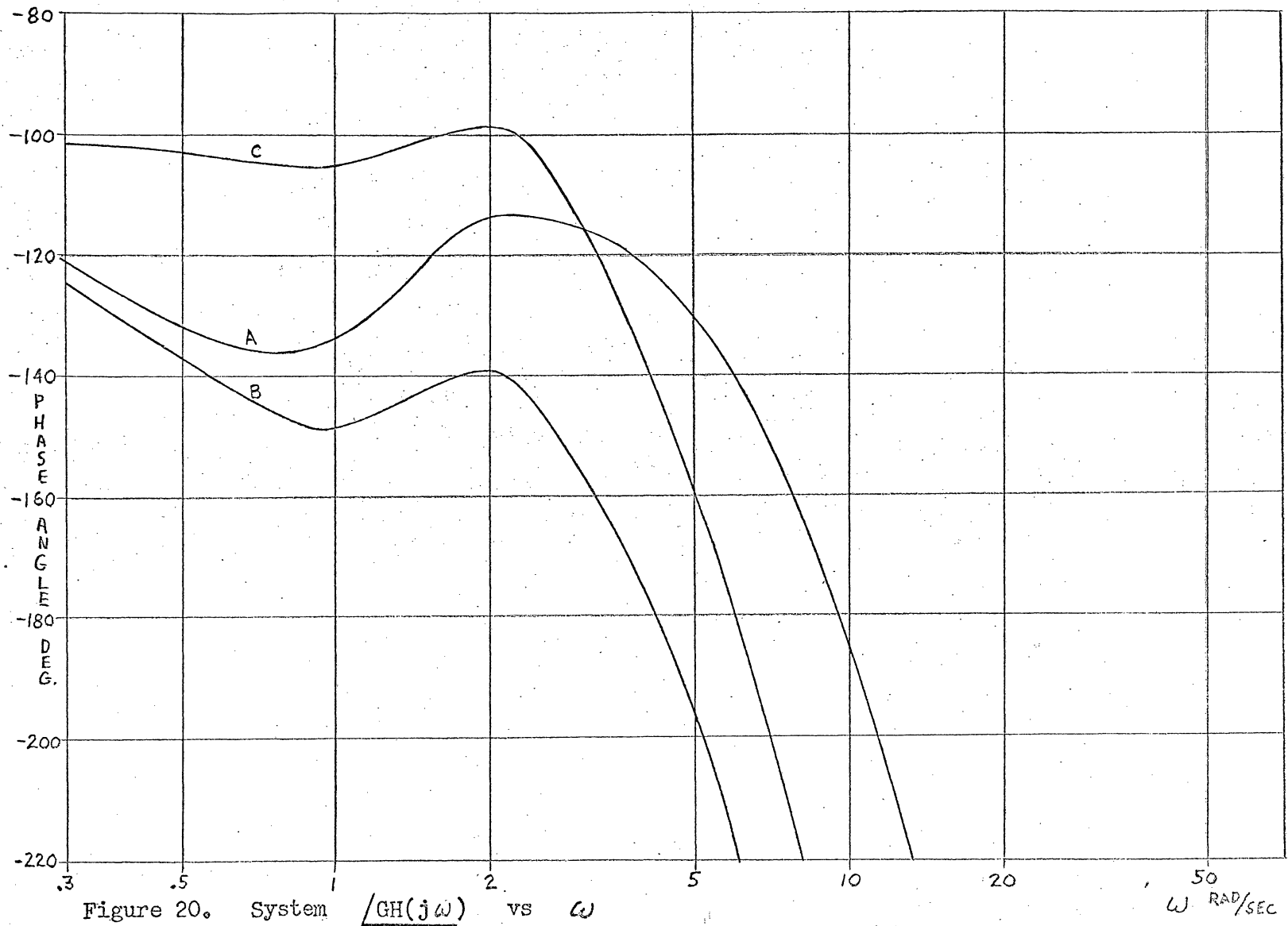
and neglecting the H_{TF} denominator,

$$\left[1 + 0,14S \right]^2_{(\zeta_2)}$$

- 2) Curve B is the same as curve A except the H_{TF} denominator is not neglected and the corrected system damping constant is taken as

$$\zeta_2 = 0.8$$





3) Curve C is the same as Curve B except the compensation of $G_c(S)$ is added and taken as,

$$G_c(S) = \frac{1 + 2S}{1 + 0.5S} \cdot \frac{1 + 0.1S}{1 + 0.02S}$$

Figure 20 is a plot of the phase angle of $GH(j\omega)$ under the same system conditions as figure 19, and the lettering of the curves correlates the $|GH(j\omega)|$ and $\angle GH(j\omega)$ as a function of the angular frequency ω .

The procedure followed considers the gain term K_{CH} as 40 db which in straight gain would be,

$$K_{CH} = 100$$

This value of K_{CH} is selected arbitrarily, simply to designate a one per unit scaling for the gain term. In other words, the actual system gain K_{CH} is the most difficult system parameter to establish quantitatively. Because of this fact, the Bode system analysis is best accomplished by looking primarily at the phase angle of $GH(j\omega)$ and determining from figures 19 and 20 the optimum system crossover frequency (ω_{co}). In addition since the bank gain term k_b is a function of the geological condition of the overburden at any time, allowance must be made in the Bode analysis for a variable gain.

Curves A and B of figure 20 correlated with figure 19 show a tendency towards marginal stability of the system if the crossover frequency were taken at,

$$\omega_{co} \approx 2 \text{ rad/sec}$$

Under this condition a loss of gain would also reflect a loss of phase margin, which is contrary to the normal axiom of reducing gain to increase phase margin and thus stability.

The reduction in system phase margin caused by the system mechanical oscillatory frequency is demonstrated by inspection of curves A and B of figure 20.

The system compensation in this example was selected to allow a system crossover frequency of,

$$\omega_{co} \approx 4 \text{ rad/sec}$$

and at the same time flatten out the dip occurring at 2 rad/sec in the phase angle of $GH(j\omega)$ as shown on figure 20.

For the system crossover frequency of 4 rad/sec in this example, the system gain at this angular frequency is shifted and re-defined as the 0 db line.

Therefore after correcting the straight line Bode curve C at the system crossover frequency, the arbitrary 28 db line is taken as the 0 db line, and consequently the system gain is identified as,

$$K_{CH} \approx 40 - 28 = 12 \text{ db}$$

Thus for this example a system gain of 12 db with a system crossover frequency of 4 rad/sec, will give protection against loss of phase margin caused by loss of system gain through either a changing overburden condition or saturation, which is the essential non-linearity of the basic motion regulators.

Although this example was selected based on the characteristics of a particular stripping shovel control system, there is good reason to believe that the techniques established in this example will carry over analogously to other such stripping shovel control systems.

VII. ACKNOWLEDGEMENTS

The author desires to express his gratitude to Dr. M. H. Hopkins for his cooperation and assistance both in class and in the preparation of this thesis.

Dr. K. G. Black and Mr. M. A. Neslin both deserve a note of thanks for their assistance in educating the author on the dynamics of the strip mining shovel.

The author is especially grateful to Mrs. Betty Blosser for her patient efforts in the typing of this thesis, and to his wife for her perserverence and assistance in the proof-reading of the manuscript.

VIII. BIBLIOGRAPHY

Literature Cited

1. Black, Dr. K. G., "Crowd-Hoist Automatic Regulator Interim Report", General Electric Company 1964.
2. Chestnut, H. and Mayer, R. W., "Servomechanisms and Regulating System Design", John Wiley & Sons, Inc., Vol. I, 1951, pp. 327-343.
3. Smith, Otto J. M., "Feedback Control Systems", McGraw-Hill Book Co., Inc., 1958, pp. 16-45 and pp. 88-111.
4. Hohn, Franz E., "Elementary Matrix Algebra", The Macmillan Co., 1959, pp. 29-42, pp. 69-71 and pp. 111-148.
5. Truxal, John G., "Automatic Feedback Control System Synthesis", McGraw-Hill Book Co., Inc., 1955, pp. 161-220.
6. Newton, G. C., Gould, L. A. and Kaiser, J. F., "Analytical Design of Linear Feedback Controls", John Wiley & Sons, Inc., 1961, pp. 10-16.
7. Cheng, D. K., "Analysis of Linear Systems", Addison-Wesley Publishing Co., Inc., 1961, pp. 52-58.
8. Cheng, D. K., "Analysis of Linear Systems", Addison-Wesley Publishing Co., Inc., 1961, pp. 58-63.
9. Millman, J. and Taub, H., "Pulse and Digital Circuits", McGraw-Hill Book Co., 1956, pp. 22-26.
10. Holl, D. L., Maple C. G. and Vinogarde, B., "Introduction to the Laplace Transform", Appleton-Century-Crofts, Inc., 1959, pp. 21-31.
11. "Handbook of Chemistry and Physics", Chemical Rubber Publishing Co., 1951, pp. 284-293.

Literature Reviewed

- Becker, R. A., "Introduction to Theoretical Mechanics",
McGraw-Hill Co., Inc., 1954.
- Black, Dr. K. G., "Crowd-Hoist Automatic Regulator Interim Report",
General Electric Company 1964.
- Cheng, D. K., "Analysis of Linear Systems", Addison-Wesley Publishing
Co., Inc., 1961.
- Chestnut, H. and Mayer, R. W., "Servomechanisms and Regulating System
Design", John Wiley & Sons, Inc., Vol. I, 1951.
- Hohn, Franz E., "Elementary Matrix Algebra", The Macmillan Co., 1959.
- Holl, D. L., Maple C. G. and Vinogarde, B., "Introduction to the
Laplace Transform", Appleton-Century-Crofts, Inc.
- Horowitz, I. M., "Synthesis of Feedback Systems", Academic Press Inc.,
1963.
- Johnson, W. C., "Mathematical and Physical Principles of Engineering
Analysis", McGraw-Hill Book Co., Inc., 1944.
- Millman, J. and Taub, H., "Pulse and Digital Circuits", McGraw-Hill
Book Co., Inc., 1956.
- Newton, G. C., Gould, L. A. and Kaiser, J. F., "Analytical Design
of Linear Feedback Controls", John Wiley & Sons, Inc., 1961.
- Smith, Otto J. M., "Feedback Control Systems", McGraw-Hill Book Co.,
Inc., 1958.
- Truxal, John G., "Automatic Feedback Control System Synthesis",
McGraw-Hill Book Co., Inc. 1955.

**The vita has been removed from
the scanned document**

X. APPENDICES

Appendix 1. Analysis Of Mechanical System

The purpose of this appendix is to show how the models and equation of section IV were generated from the basic analysis of the mechanical system's dynamics,

Figure 21 shows a model of the mechanical system. Although it is vastly simplified from the true physical world representation, it is to all intents sufficient for the purpose. The drawing shows how mechanical oscillations due to the interactions between the hoist drive (hoist motor, gears and drum) and the driven mass (dipper and dirt) are introduced into the hoist motion through the hoist rope. The hoist rope is a steel cable with a certain coefficient of elasticity.

Since, it is preferable with a rotating mechanical drive to consider the mechanical system in rotational terms, the analogous system model of figure 22 supplants the original model of figure 21. In other words, the elastic rope and rigid shaft is replaced with a rigid rope and an elastic shaft in order to represent the spring constant as a torsional rather than a straight line force representation.

Based on the model of figure 22, the following differential equations will yield the properties of the torsional analog.

Breaking the elastic shaft at its mid-point, and then considering the inertial effects of motor (M) and load (L) will yield,

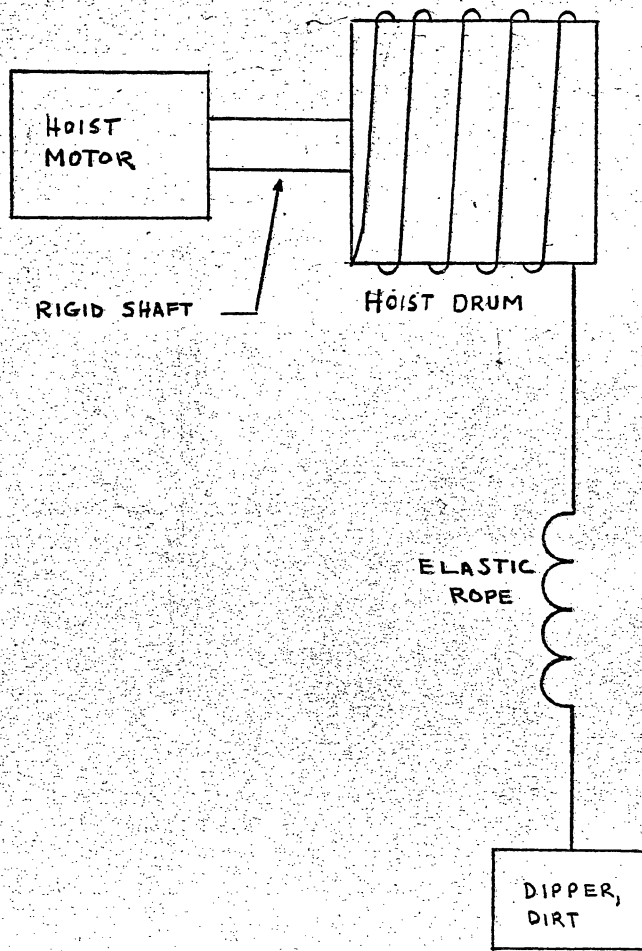


Figure 21. Mechanical System - Force

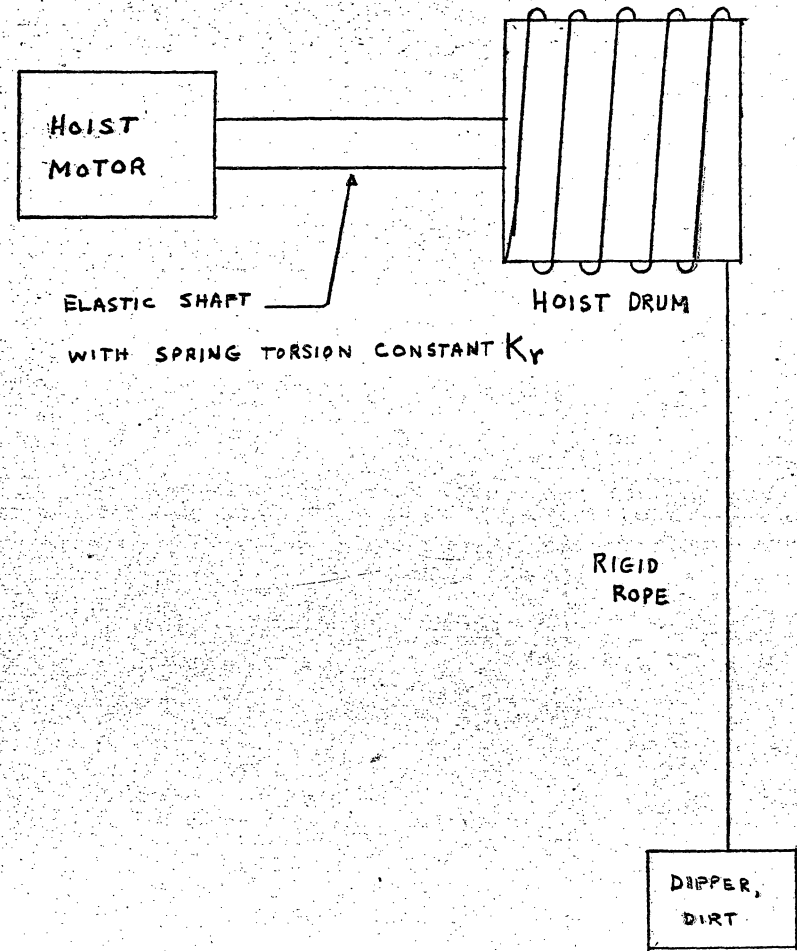


Figure 22. Mechanical System - Torsional

$$J_M \ddot{\theta}_M + D(\dot{\theta}_M - \dot{\theta}_L) + K_r(\theta_M - \theta_L) = 0$$

$$J_L \ddot{\theta}_L - D(\dot{\theta}_M - \dot{\theta}_L) + K_r(\theta_M - \theta_L) = 0$$

where, D = mechanical system damping constant

K_r = spring torsion constant

J_M = motor inertia

J_L = load inertia

For the frequency of oscillation of this mechanical system, set D equal to zero, and consider the characteristic equation of the resulting 2×2 determinant,

$$\begin{vmatrix} (J_M s^2 + K_r) & -K_r \\ -K_r & (J_L s^2 + K_r) \end{vmatrix} = 0$$

which yields,

$$J_M J_L s^4 + (J_M + J_L) K_r s^2 = 0$$

therefore,

$$s^2 + \frac{J_M + J_L}{J_M J_L} K_r = 0$$

let $s = j\omega_0$

where, ω_0 is the oscillatory mechanical system frequency this yields,

$$\omega_0^2 = \frac{J_M + J_L}{J_M J_L} K_r$$

which is the expression that Dr. Black has in his report (section IV).

What this really yields is a means of experimentally determining the constant K_r from observation of the oscillatory frequency present in the mechanical system. Similarly, a good approximation of the damping constant (D) can be obtained from actual observation of the shovel's mechanical system when subjected to a disturbance.

The block diagram of the motor and mechanical system figure 4 section IV is a direct representation of the system differential equations given in this appendix. If it is desired to reduce the block diagram of figure 4 page 16, to obtain the simplified model of figure 5, page 17, it is easily done by a determinantal solution from the matrix expression,

$$\begin{bmatrix} 1 & (D + \frac{K_r}{S}) & 0 \\ \frac{-1}{J_M S} & 1 & \frac{1}{J_L S} \\ 0 & -(\frac{D + K_r}{S}) & 1 \end{bmatrix} \begin{bmatrix} e_1 \\ e_2 \\ e_3 \end{bmatrix} = \begin{bmatrix} I_1 \\ I_2 \\ -I_3 \end{bmatrix}$$

Where, from left to right on figure 4, neglecting the V_g input, the summing junction inputs are I_1 , I_2 and I_3 (T_L), and e_1 , e_2 and e_3 are the errors after these summing junctions.

The determinantal solutions, where the delta is the determinant of the 3 x 3 matrix, are

with $I_2 = I_3 = 0$,

$$G_b = \frac{\omega_M}{I_1} = \frac{e_1}{I_1} \frac{1}{J_M S}$$

with $I_1 = I_2 = 0$

$$G_g = \frac{1}{G_b} \frac{\omega_M}{I_3} = \frac{1}{G_b} \frac{e_1}{I_3} \frac{1}{J_M S}$$

Appendix 2. Analysis of System H_t

From section IV equation 4.6 says that,

$$H_t = \frac{K_v (1 - \zeta_1) 2 T_o S}{G_f (1 + T_o S)^2}$$

A simplification of the transfer G_f from section VA1 is given by,

$$G_f \approx \frac{k_f (1 + T_f S)}{(1 + b S + a S^2)}$$

Based on this assumption,

$$H_t = \frac{K_w S (1 + b S + a S^2)}{(1 + T_f S) (1 + T_o S)^2} \quad \text{A2.1}$$

$$\text{where, } K_w = \frac{K_v (1 - \zeta_1) T_o}{k_f}$$

Now, consider the block diagram of figure 23 which has the following transfer function,

$$H_t = K_m K_t S \left[\frac{k_1 (1 + T_1 S)}{1 + T_3 S} - \frac{k_2 (1 + T_2 S)}{1 + T_4 S} \right]$$

$$\text{where } K_w = K_m K_t$$

This resolves to equation A2.2 as follows

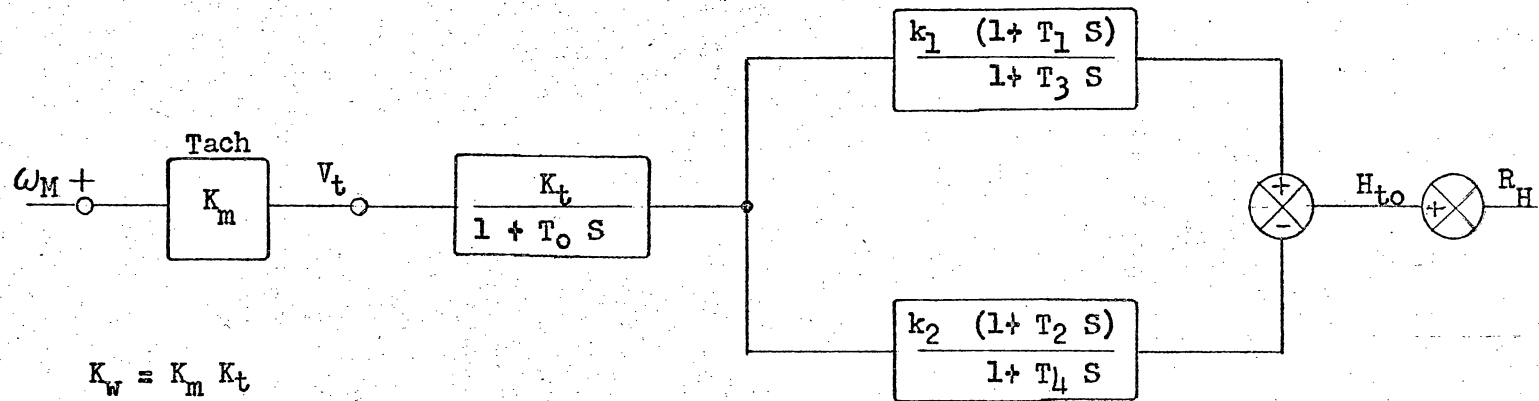


Figure 23. H_t Feedback Network $\frac{\Delta H_{to}}{\Delta \omega_M}$

$$H_t = K_m \frac{K_t S}{1 + T_o S} \left[\frac{(k_1 - k_2) + [k_1 (T_1 + T_4) - k_2 (T_2 + T_3)] S}{(1 + T_3 S) (1 + T_4 S)} + \frac{(k_1 T_1 T_4 - k_2 T_2 T_3) S^2}{(1 + T_3 S) (1 + T_4 S)} \right] \quad \text{A2.2}$$

Since equations A2.1 and A2.2 are to be equal, the following conditions are met,

- 1) $k_1 - k_2 = 1$
- 2) $k_1 (T_1 + T_4) - k_2 (T_2 + T_3) = b$
- 3) $k_1 T_1 T_4 - k_2 T_2 T_3 = a$

Also, arbitrarily let,

$$T_3 = T_o \quad T_4 = T_f \quad k_1 = 2 \quad k_2 = 1$$

Then for these conditions,

- 2) $2T_1 - T_2 = b + T_o - 2T_f$
- 3) $2T_f T_1 - T_o T_2 = a$

Now simultaneous solution by determinants yields,

$$T_1 = \frac{a - (b + T_o - 2T_f) T_o}{2 (T_f - T_o)} \quad \text{A2.3}$$

$$T_2 = \frac{a - (b + T_o - 2T_f) T_f}{(T_f - T_o)} \quad \text{A2.4}$$

If the H_t feedback network is kept in the most general form, two equations from equations 2) and 3) result,

$$k_1 T_1 - k_2 T_2 = b + k_2 T_3 - k_1 T_4$$

$$k_1 T_4 T_1 - k_2 T_3 T_2 = a$$

Now simultaneous solution by determinants yields,

$$T_1 = \frac{a - (b + k_2 T_3 - k_1 T_4) T_3}{k_1 (T_4 - T_3)} \quad \text{A2.5}$$

$$T_2 = \frac{a - (b + k_2 T_3 - k_1 T_4) T_4}{k_2 (T_4 - T_3)} \quad \text{A2.6}$$

When K_w , T_f , T_o , a and b are known from the system study, these equations will be required along with those equations in section VB1 in order to resolve the H_t feedback network for the particular system parameters.

Appendix 3. H_t Time Domain Linear Analysis Response

The purpose of this appendix is to develop a general solution for the time response of the H_t feedback network to a given ramp input. This is necessary in order to insure that the saturation levels of the operational amplifiers are not exceeded. In other words, the H_t feedback network is desired to be linear.

The H_t network of section VB1 and appendix 2 may be represented in Laplace notation as shown in figure 24.

The following assumptions are made:

- 1) $V_t(t) = A t$; $V_t(S) = \frac{A}{S^2}$
- 2) $k_t k_o = K_t$
- 3) initial conditions $V_t(t) = 0$ at $t = 0$

For solution of $V_1(t)$,⁽¹⁰⁾

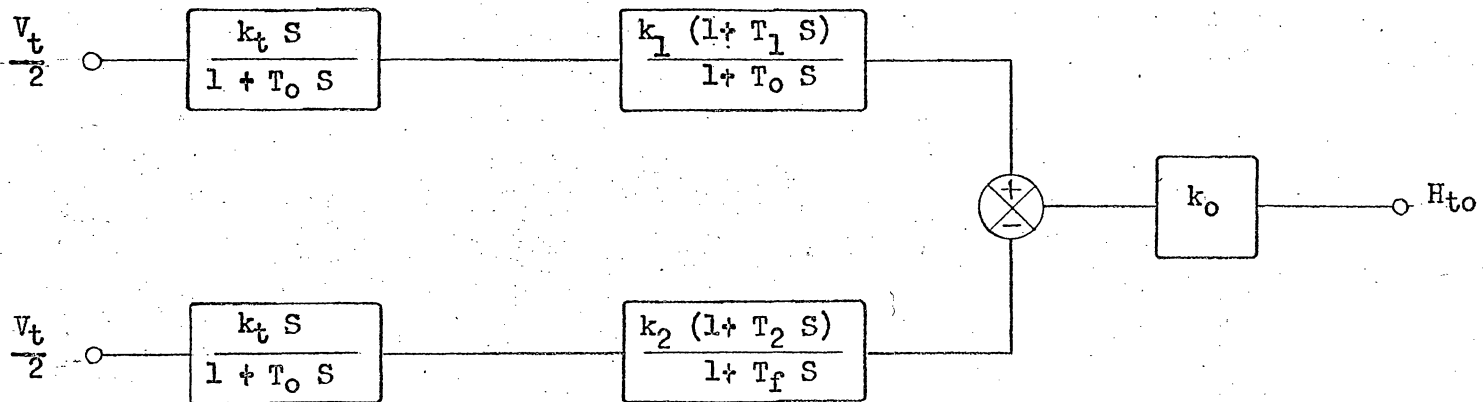
$$V_1(S) = \frac{A}{2 S^2} \frac{k_t S}{1 + T_o S} = \frac{A}{2} k_t \frac{1}{S(1 + T_o S)} = \frac{A k_t}{2} \left[\frac{1}{S} - \frac{1}{S + \frac{1}{T_o}} \right]$$

Taking inverse Laplace,⁽¹¹⁾

$$V_1(t) = \frac{A k_t}{2} \left[1 - e^{-t/T_o} \right] \tag{A3.1}$$

For solution of $V_2(t)$,

$$V_2(S) = \frac{A}{2 S^2} \frac{k_t S}{1 + T_o S} \frac{k_1 (1 + T_1 S)}{1 + T_o S} = \frac{A k_t k_1}{2} \frac{1 + T_1 S}{(1 + T_o S)^2}$$



where, $k_t k_o = K_t$

Figure 24. H_t Branch Circuit Model

By partial fraction expansion, (10)

$$V_2 (S) = \frac{A k_t k_1}{2} \left[\frac{1}{S} - \frac{1}{S + \frac{1}{T_o}} + \frac{\frac{T_1 - T_o}{T_o^2}}{\left(S - \frac{1}{T_o}\right)^2} \right]$$

Taking inverse Laplace (11)

$$V_2 (t) = \frac{A k_t k_1}{2} \left[1 - e^{-t/T_o} + \frac{(T_1 - T_o)}{T_o^2} t e^{-t/T_o} \right] \quad A3.2$$

For solution of $V_3 (t)$,

$$V_3 (S) = \frac{A}{2} \frac{k_t S}{S^2 (1 + T_o S)} \frac{k_2 (1 + T_2 S)}{1 + T_f S} = \frac{A k_t k_2 (1 + T_2 S)}{2 (1 + T_o S) (1 + T_f S)}$$

By partial fraction expansion, (10)

$$V_3 (S) = \frac{A k_t k_2}{2} \left[\frac{1}{S} + \frac{\frac{T_2 - T_f}{T_f - T_o}}{S + \frac{1}{T_f}} - \frac{\frac{T_2 - T_o}{T_f - T_o}}{S + \frac{1}{T_o}} \right]$$

Taking inverse Laplace, (11)

$$V_3 (t) = A k_t k_2 \left[1 + \frac{\{T_2 - T_f\} e^{-t/T_f} - \{T_2 - T_o\} e^{-t/T_o}}{T_f - T_o} \right] \quad A3.3$$

For solution of $H_{to}(t)$,

$$H_{to}(t) = \left[V_2(t) - V_3(t) \right] k_o$$

substituting for $V_2(t)$ and $V_3(t)$ yields equation A3.4,

$$H_{to}(t) = \frac{A k_t k_o}{2} \left[(k_1 - k_2) + \left[\frac{(T_1 - T_o) k_1}{T_o^2} t + \frac{(T_2 - T_o) k_2 - k_1}{T_f - T_o} \right] e^{-t/T_o} - \frac{(T_2 - T_f)}{T_f - T_o} e^{-t/T_f} \right] \quad \text{A3.4}$$

where normally, $T_2 > T_f > T_1 > T_o$

$$k_1 > k_2$$

Appendix 4. General Form Of Motion Transfer Functions

The purpose of this appendix is to identify in general form the motion transfer functions of figure 12, page 30 for the crowd and hoist motions. To help correlate figure 12 with the physical system, the fixed plant will be listed separately from the control system transfer functions, and the correct units for the gain term of the transfer function will be given.

Fixed Plant (Ward-Leonard Loop)

$$G_5 = \frac{K_g}{1 + T_g S} \quad \frac{\text{volts}}{\text{amp turn}}$$

$$G_6 = \frac{1}{R_A (1 + T_A S)} \quad \frac{1}{\text{ohm}}$$

$$G_7 = K_T \quad \frac{\text{lb - ft}}{\text{amp}}$$

$$G_8 = \frac{1}{J S} \quad \frac{\text{rad/sec}}{\text{lb - ft}}$$

$$H_5 = K_{SF} \quad \frac{\text{amp turn}}{\text{amp}}$$

$$H_6 = K_V \quad \frac{\text{CEMF volts}}{\text{rad/sec}}$$

Control system

$$G_1 = \frac{K_1}{1 + T_1 S} \quad \begin{array}{l} \text{amp turn} \\ \text{amp turn} \end{array}$$

$$G_2 = \frac{K_2}{1 + T_2 S} \quad \begin{array}{l} \text{volt} \\ \text{amp turn} \end{array}$$

$$G_3 = K_3 \quad \begin{array}{l} \text{amp turn} \\ \text{volt} \end{array}$$

$$G_4 \approx \frac{K_4}{(1 + T_f S)(1 + T_q S)} \quad \begin{array}{l} \text{amp turn} \\ \text{amp turn} \end{array}$$

Note: G_4 actually consists of four gain blocks each with its own gain and time constant, however it may be simplified to the transfer function given without unduly jeopardizing the integrity of the system. G_4 is the generator field exciter.

$$H_1 = \frac{K_C S}{1 + T_C S} \quad \begin{array}{l} \text{amp turn/sec} \\ \text{volt} \end{array}$$

$$H_2 = K_{VR} \quad \begin{array}{l} \text{amp turn} \\ \text{volt} \end{array}$$

$$H_3 = K_{VC} \quad \frac{\text{amp turn}}{\text{volt}}$$

$$H_4 = K_{CL} R_{CF} (1 + T_{CF}S) \quad \frac{\text{amp turn}}{\text{amp}}$$

As shown on figure 11, page 28 the crowd motion is not in current limit, and therefore for the area of interest of this thesis the G_1 , H_1 , H_3 and H_4 crowd motion gain blocks are not required.

It is not intended in these generalized motion transfer functions to imply that any of the actual numbers for a particular gain block are the same for both the hoist and crowd motions, normally they are different.

AN AUTOMATIC CROWD-HOIST REGULATOR
FOR THE STRIP MINING INDUSTRY

ABSTRACT

The object of this thesis is to establish the necessary design criteria for a number of special feedback networks which were required to allow the final development of the Strip Mining Industry's first Automatic Crowd-Hoist Regulator.

The introduction considers the purpose and needs for such a regulator by briefly outlining the present manual dipper loading operation.

Section IV and Appendix 1 presents the analytical system requirements which are basically determined from an analysis of the system's inherent mechanical oscillatory frequency.

Section VA is concerned with the development of the hoist and crowd motion transfer functions which are necessary to accomplish the stability analysis of the system. A general determinantal solution is obtained based on linear analysis to allow expression of the motion transfer functions as a factored polynomial.

In section VB, the development of the necessary Crowd-Hoist feedback circuits is accomplished in terms of the system parameters defined from the analysis of the oscillatory mechanical system.

Section VIA outlines the procedures to be followed in going from the basic mechanical system parameters to the specific control system hardware.

The general requirements for a Bode analysis of the system GH is defined in section VIB, including the general procedures to follow in the utilization of the two lead compensation circuits provided.

William A. DeLorme